Simulazioni quantistiche con gas atomici ultrafreddi

Gabriele Ferrari

Pitaevskii Center for Bose-Einstein Condensation

INO-CNR and Physics Department, University of Trento, Italy

Workshop INFN CSN 4 & 5

Quantum Technologies (Computing, Sensing & Simulation)

Torino, June 8th, 2023

Quantum simulation?

Gauge theories constitute the fundamental building blocks of the Standard Model of high-energy physics (HEP).

...but a lot of fundamental problems are still open!

The QCD phase diagram is largely unknown:
Exotic fermionic superfluidity? Dynamics of deconfined quarks?
(relevant e.g. for dense neutron stars and heavy-ion collisions)

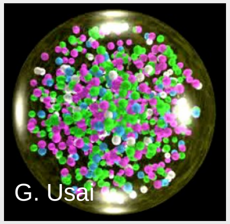

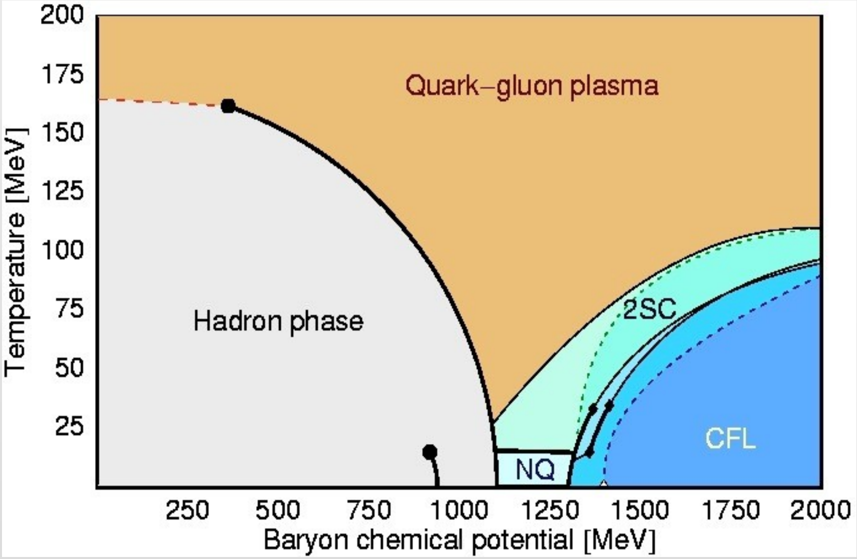

This problem is extremely difficult for any classical hardware!

You need a quantum simulator!!!

R. P. Feynman,
Int. J. Theor. Phys. (1982).

Quantum simulation?

sistemi fisici e modelli teorici difficilmente accessibili a livello sperimentale vengono studiati attraverso le loro analogie con le proprietà di altri sistemi realizzabili e controllabili accuratamente in sistemi table-top di laboratorio.

R. P. Feynman, International Journal of Theoretical Physics 21, 467 (1982)

Strumento efficace nello studio di problemi di materia condensata:

- trasporto superfluidi su reticoli,
- ordine VS disordine,
- equazioni di stato per gas quantistici fortemente interagenti.

Cosa serve? un sistema quantistico "ingegnerizzabile" e misurabile

Ultracold atoms

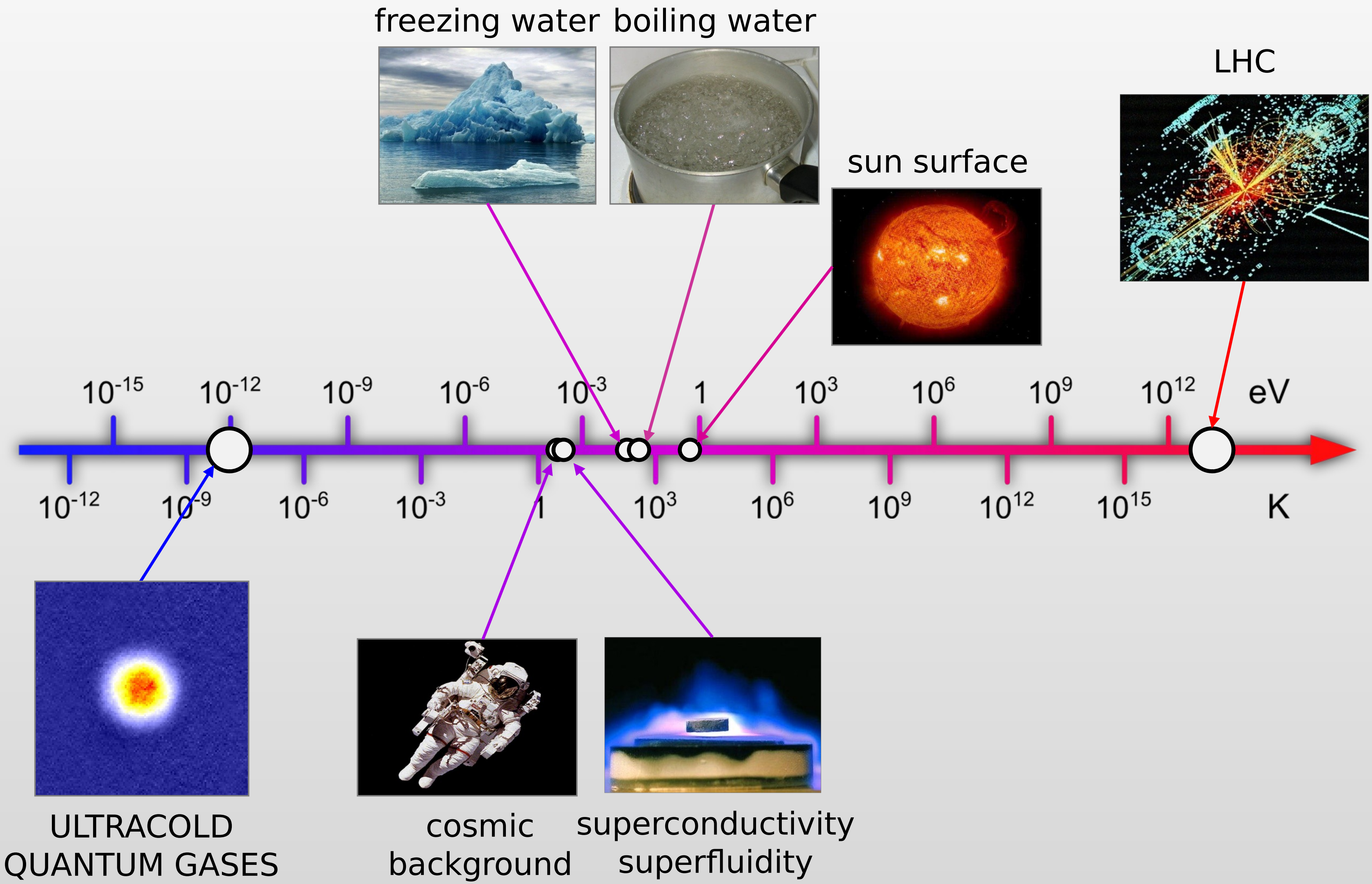

Many control knobs for realizing Hamiltonians in the lab:

Bosons and fermions
Temperature & density
Interactions
Optical lattices
Dimensionality & Topology
Mixtures of atoms and spins
Coherent coupling among spin states
Long-range interactions

Many detection capabilities:

direct imaging (real space and momentum space)
correlation functions
excitation spectra
dynamics (transport)
thermodynamics

Ultracold atoms are perfect quantum simulators for:

Quantum phase transitions	M. Greiner et al., Nature (2002)
	A. Zenesini et al., PRX (2023)
Fermi-Hubbard model	R. Jördens et al., Nature (2008)
Fermionic superfluidity	M. Zwirlein et al., Nature (2005)
Disordered systems	G. Roati et al., Nature (2007)
Relativistic dispersion	L. Tarruell et al., Nature (2012)
Higgs mechanism	M. Endres et al., Nature (2012)
Kibble-Zurek mechanism	G. Lamporesi et al., Nat. Phys. (2013)

....and much more

Studio di fermioni a molte componenti in presenza di campi di gauge

L. Fallani (LENS-Firenze)

Gas di fermioni ultrafreddi di ^{173}Yb: simmetria di interazione SU(N) e controllo coerente

- spin nucleare e stato elettronico

Realizzazione di campi di gauge in reticoli

- ottici attraverso interazioni indotte da laser

Realizzazione di prototipi di teorie di gauge

- su reticolo (quantum link models)

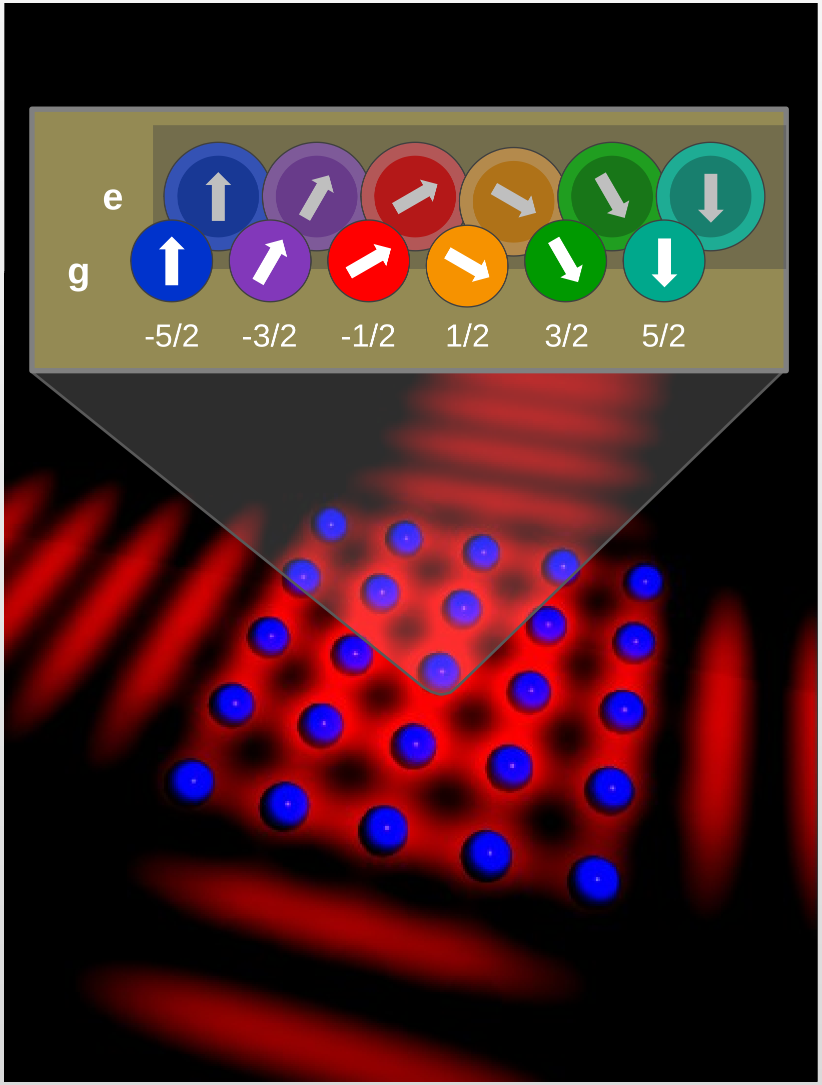

Campi di gauge statici

Campo abeliano statico U(1), equivalente
ad un campo magnetico di background in QED

Il campo magnetico «sintetico» è generato da un laser in un processo di «laser-assisted tunnelling» in cui la fase del laser viene impressa sulla funzione d'onda atomica (imprinting del potenziale vettore **A**)

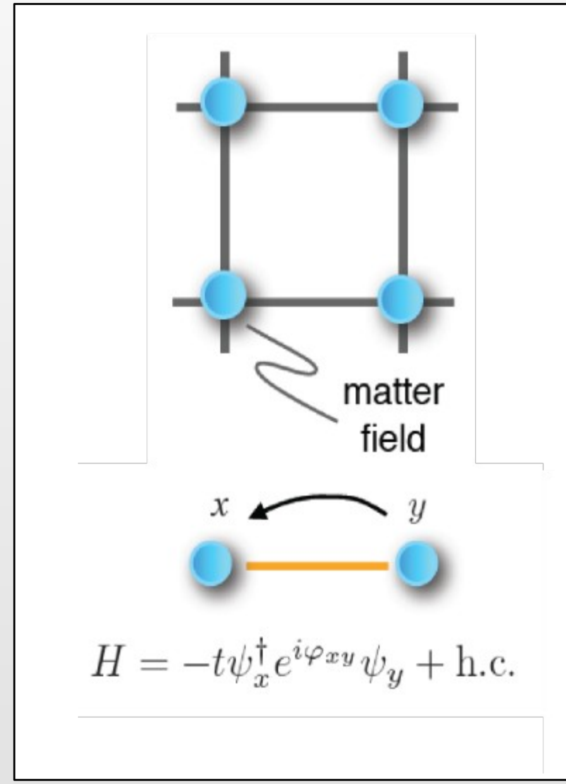

Aharonov-Bohm geometric phase

$$\psi \to e^{i\phi}\psi$$

$$\phi = 2\pi \frac{\Phi}{\Phi_0}$$

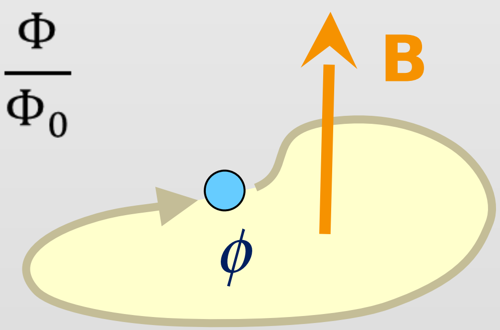

J. Dalibard et al., Rev. Mod. Phys. **83**, 1523 (2011)
N. Goldman et al., Rep. Prog. Phys. **77**, 126401 (2014)

Realizzazione di un’«extradimensione»:

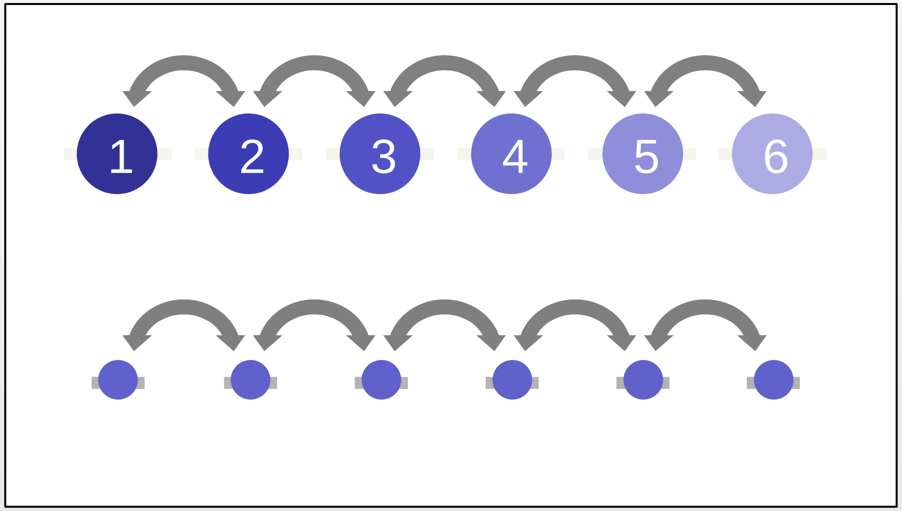

Accoppiamento coerente fra stati interni:

$$H = -\Omega \sum_m \left(c_m^\dagger c_{m+1} + h.c.\right)$$

Hopping fra siti primi vicini di un reticolo:

$$H = -t \sum_j \left(c_j^\dagger c_{j+1} + h.c.\right)$$

Campi di gauge statici U(1) con extradimensioni:

Realizzazione minimale di una "dimensione sintetica" eccitando il grado di libertà elettronico con transizione ottica ultrastretta (elevati tempi di coerenza >100 ms).

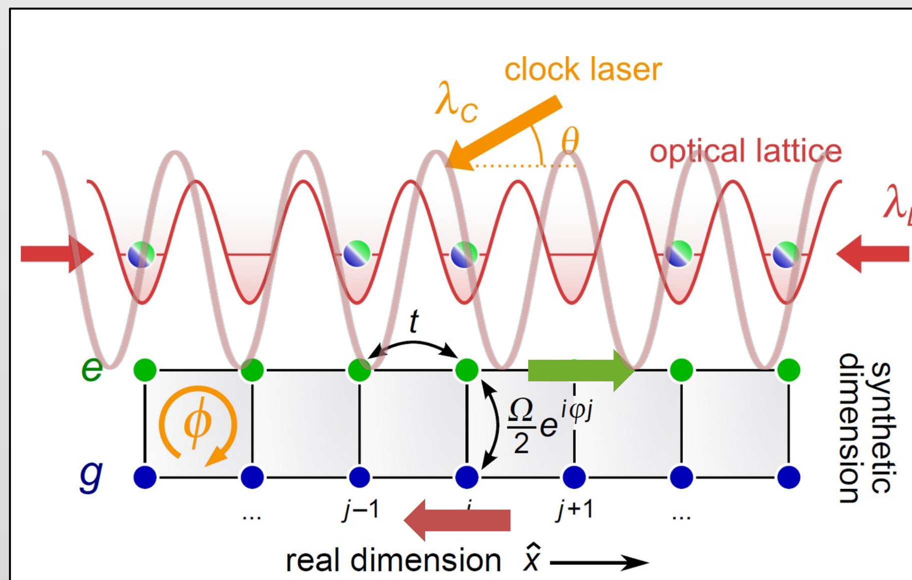

Kibble-Zurek mechanism: producing vortices via temperature quenches

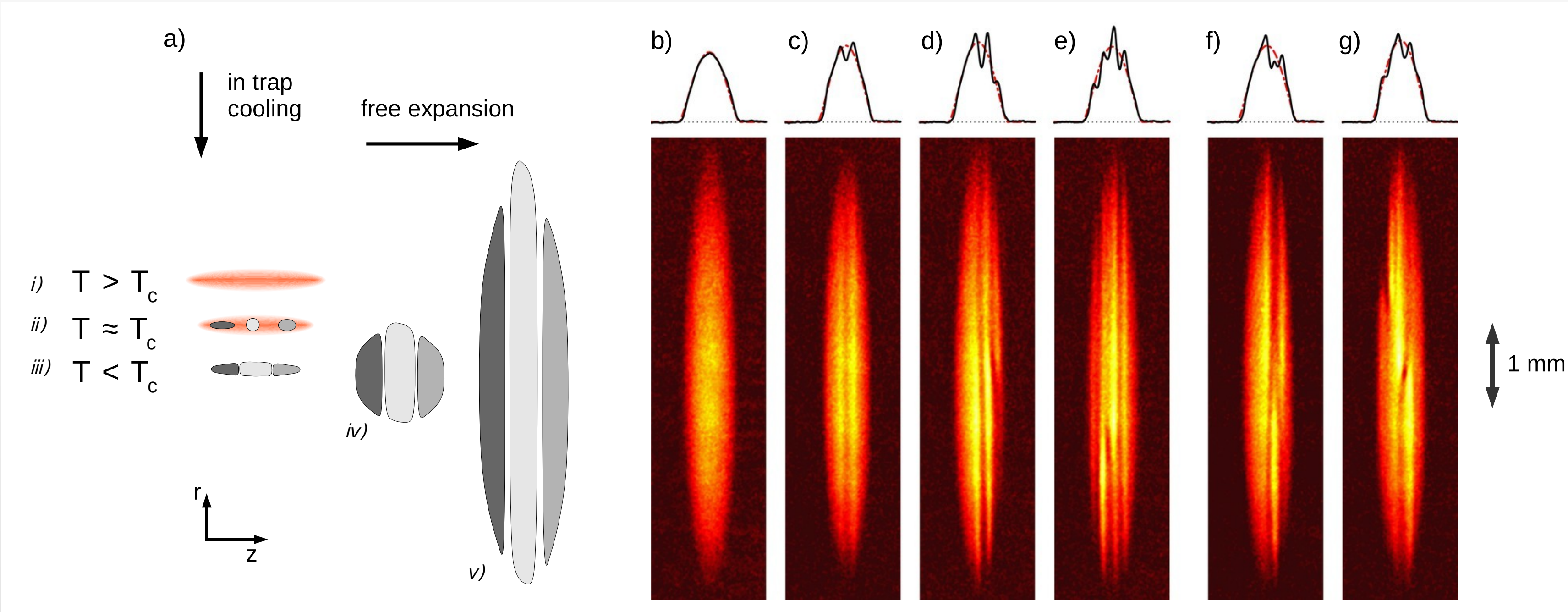

slow cooling → fast cooling

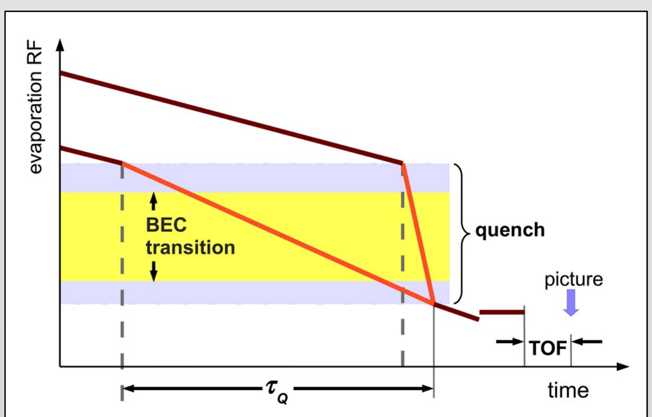

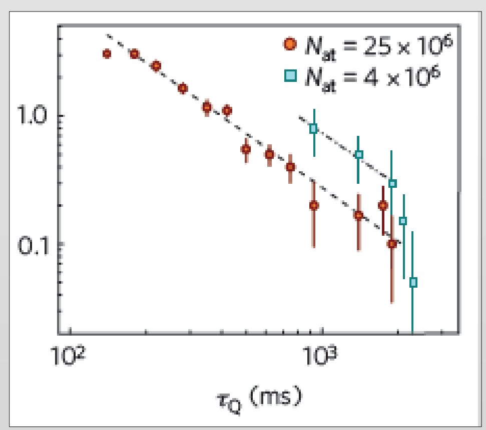

Power-law scaling of defect number vs. quench time

Lamporesi *et al.*, Nature Physics **9**, 656 (2013)

Resonantly-coupled spinor condensates

Spinor condensate is a BEC populating

many internal states, eg. Zeeman states

$$\zeta = \begin{pmatrix} \sqrt{n_{+1}} e^{i\theta_{+1}} \\ \sqrt{n_0} e^{i\theta_0} \\ \sqrt{n_{-1}} e^{i\theta_{-1}} \end{pmatrix}$$

Spin-orbit coupling

- main goal: realize and study **supersolids**, phases exhibiting crystalline spatial order and long-range coherence
- Result from the interplay of contact interaction and the S-O coupling

Rabi coupling

- main goal: produce vortex molecules, i.e. bound states of orbital vortices in the BEC spin conponents
- Vortex molecules present **analogies with quark confinement**

Resonantly-coupled spinor condensates

Generation of topological defects (domain walls on the relative phase, formally similar to the kink in the sine-Gordon field theory)

$$\boldsymbol{\zeta} = \begin{pmatrix} \sqrt{n_{+1}}e^{i\theta_{+1}} \\ \sqrt{n_0}e^{i\theta_0} \\ \sqrt{n_{-1}}e^{i\theta_{-1}} \end{pmatrix}$$

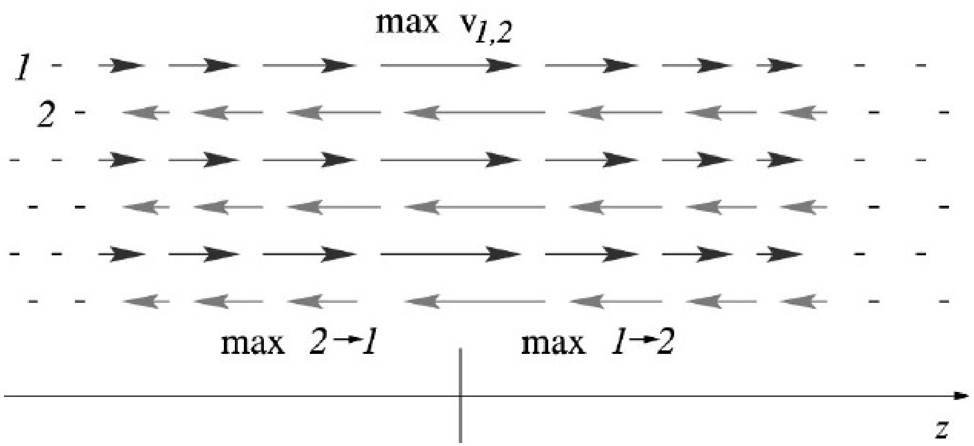

$$\varphi_A \equiv \varphi_1 - \varphi_2 = 4 \arctan e^{kz}, \quad k^2 = \frac{m\Omega}{\hbar} \frac{n}{\sqrt{n_1 n_2}}$$

$$E[\varphi_1, \varphi_2] = \int d^3\boldsymbol{x} \left[\frac{\hbar^2}{2m} [n_1 (\nabla \varphi_1)^2 + n_2 (\nabla \varphi_2)^2] - \hbar \Omega \sqrt{n_1 n_2} \cos(\varphi_1 - \varphi_2) \right]$$

Domain walls of relative phase in two-component BECs

D. T. Son & M. A. Stephanov, Phys. Rev. A 65, 063621 (2002)

Rabi-coupled system

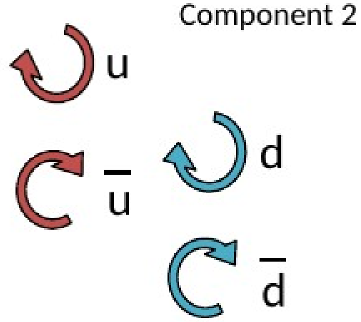

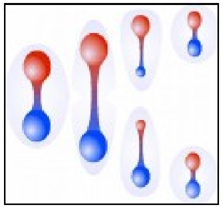

Baryons

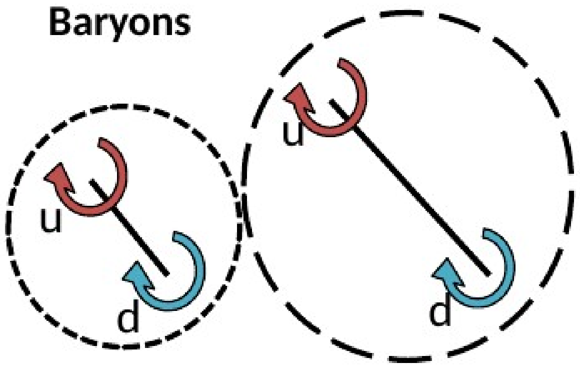

Mesons

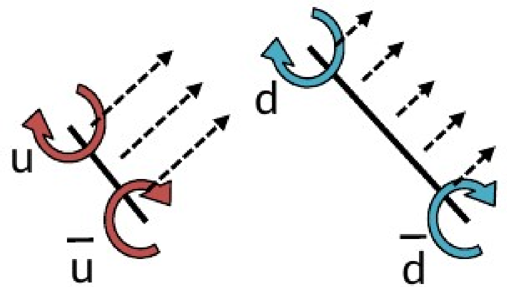

Baryon dynamics

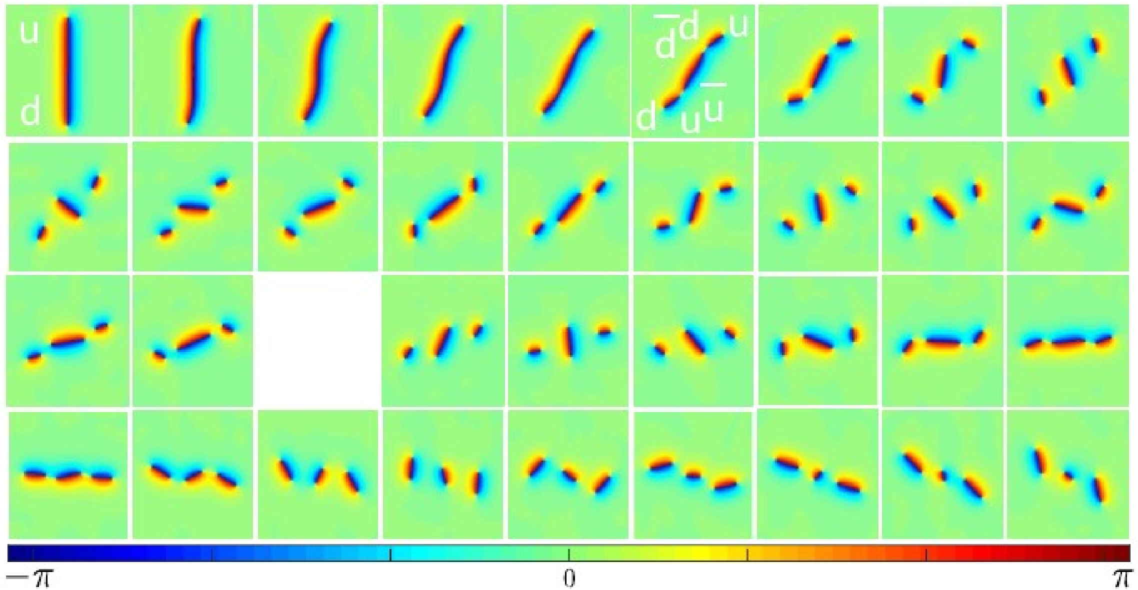

Meson dynamics

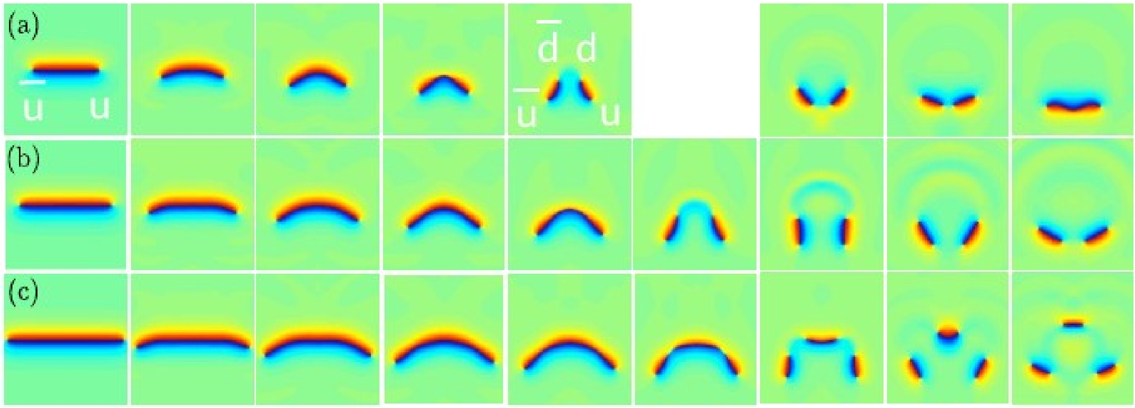

Tylutki et al., PRA **93**, 043623 (2016) Eto and Nitta, PRA **97**, 023613 (2018)

Imaging a spinor wavefunction

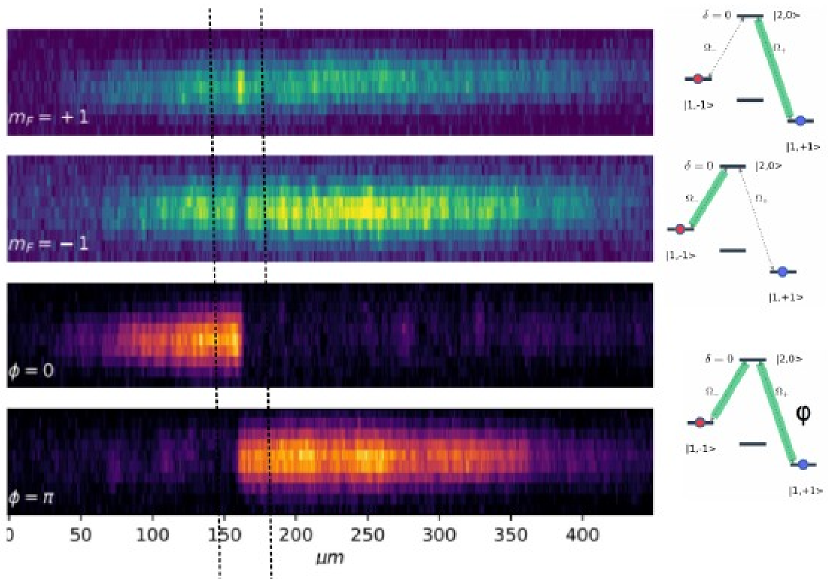

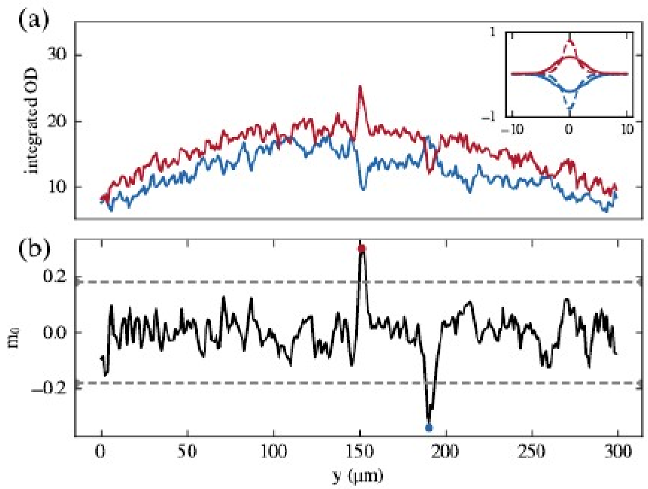

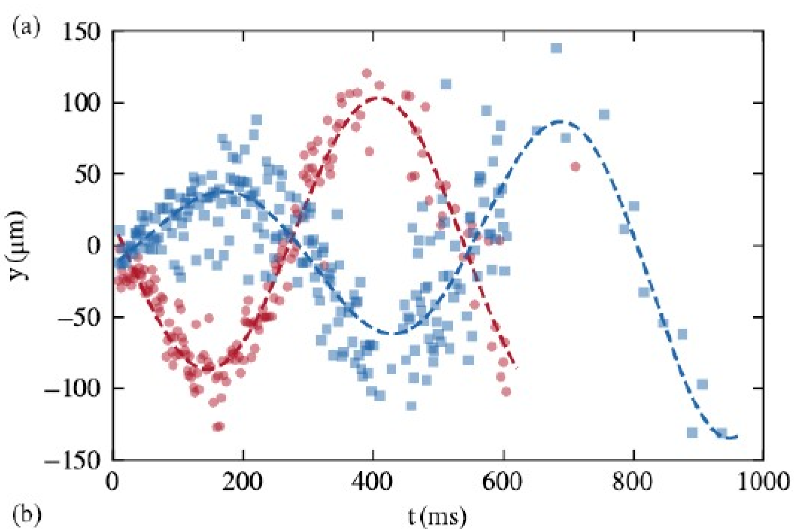

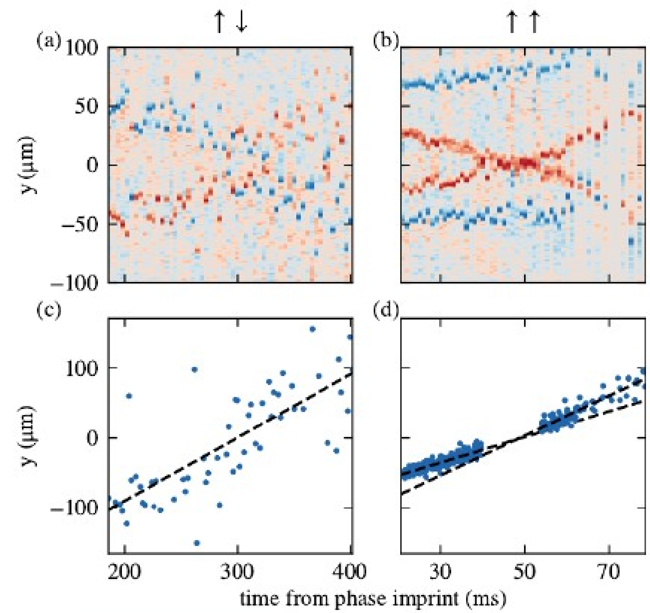

A. Farolfi et al., Phys. Rev. Lett. 125, 030401 (2020)

Phase imprint of the domain wall

$$U_0 = \frac{\hbar \gamma I_0}{24 I_S}\left[\left(\frac{1}{\delta_{1/2}} + \frac{2}{\delta_{3/2}}\right) - g_F m_F \sqrt{1-\epsilon^2}\left(\frac{1}{\delta_{1/2}} - \frac{1}{\delta_{3/2}}\right)\right]$$

= 0

spin-dependence

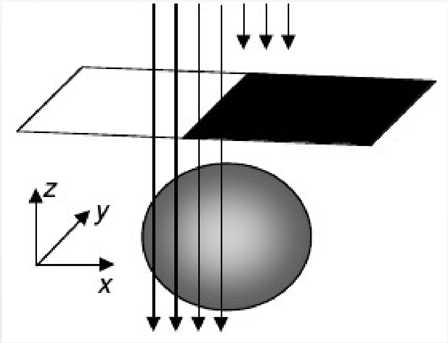

The laser frequency is chosen to introduce a phase shift proportional to the m_F state

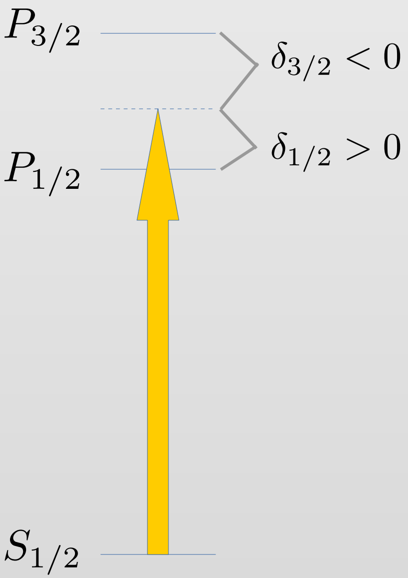

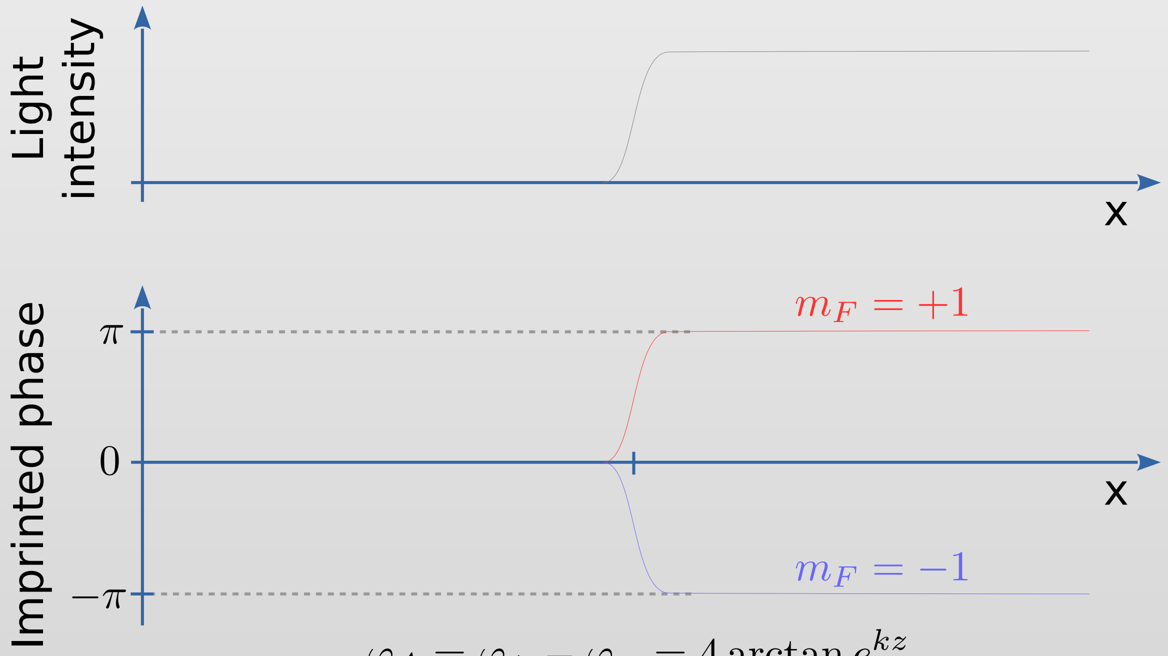

$$\varphi_A = \varphi_+ - \varphi_- = 4 \arctan e^{kz}$$

Measurement of the relative phase

Uniform illumination

Razor blade in

blade position

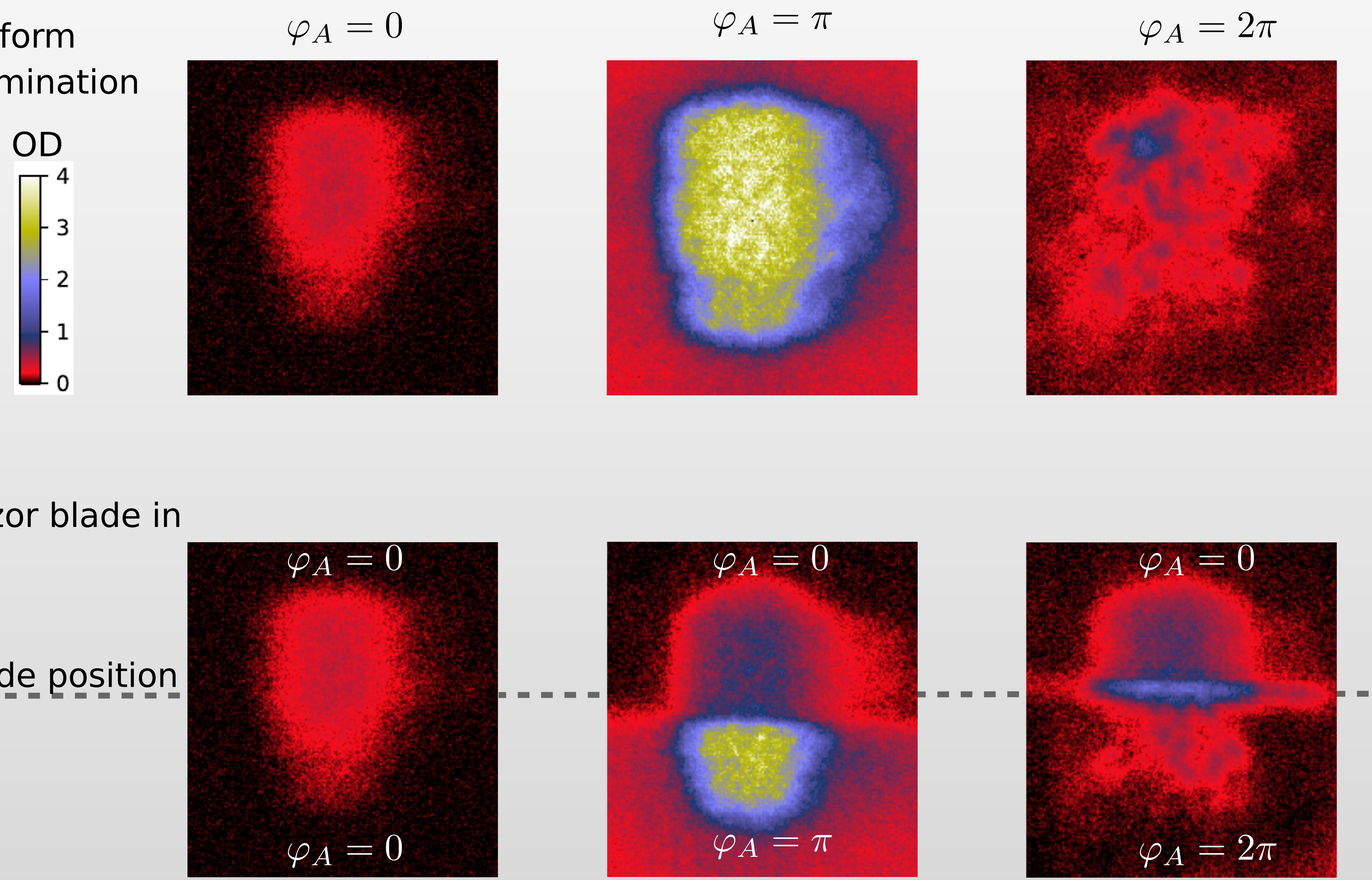

Time evolution of the domain wall

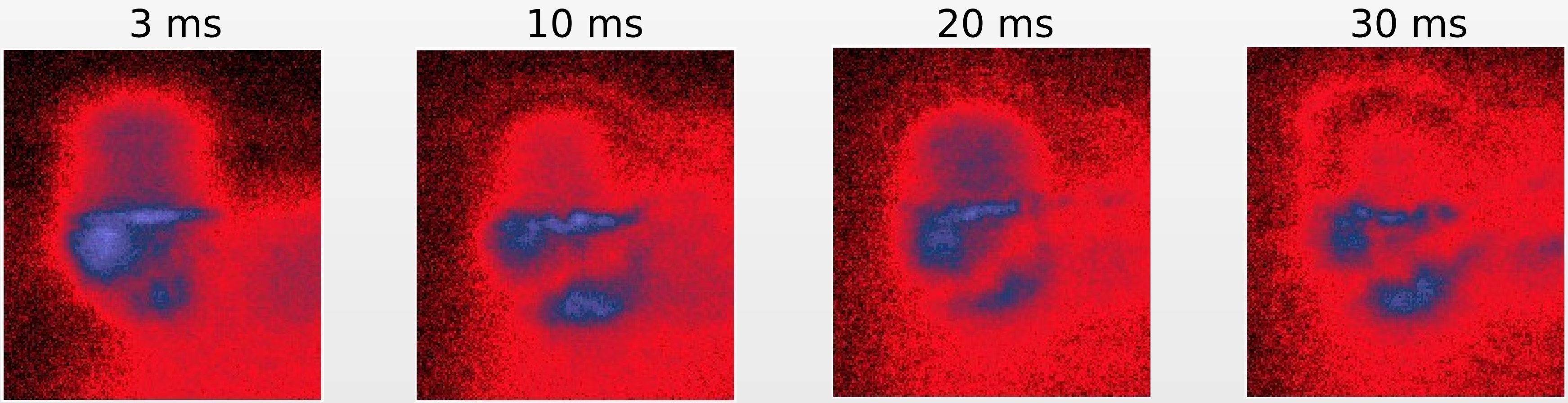

Numerical simulation:

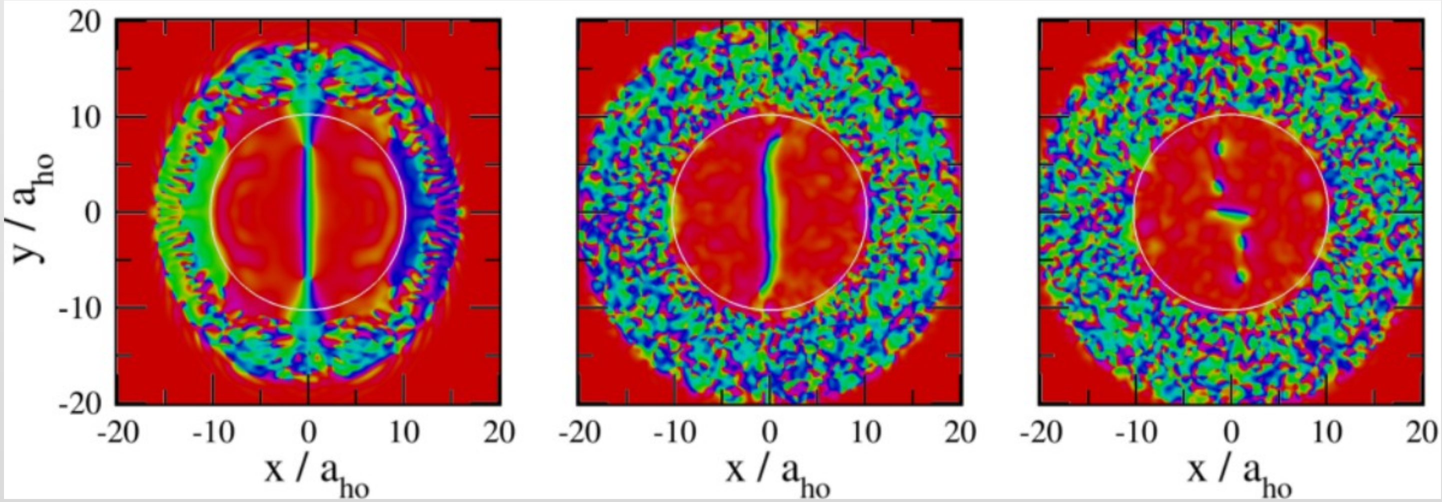

A. Gallemí et al., Phys. Rev. A 100, 023607 (2019)

Quantum simulations with spin mixtures

SUPERFLUIDITY MAGNETISM

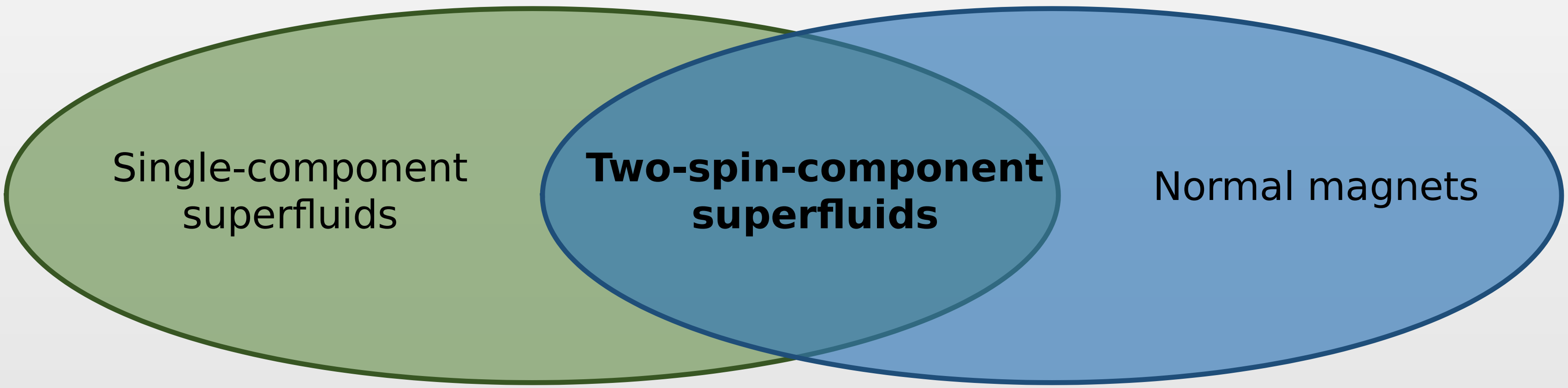

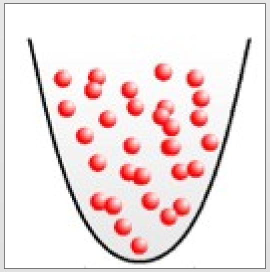

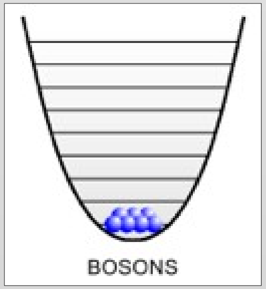

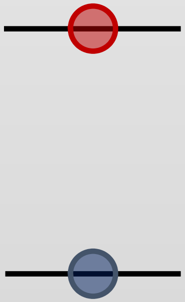

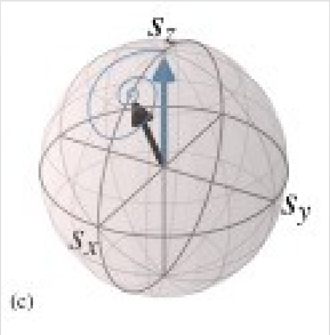

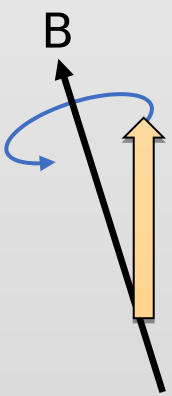

Miscibility

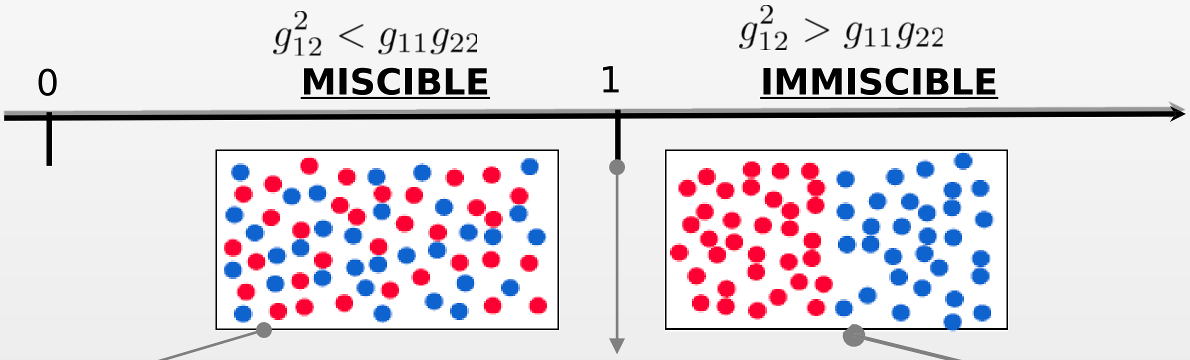

Maximum overlap

Close to the (im)miscible transitions:
Spin channel is much less energetic than the density one

Phase separation

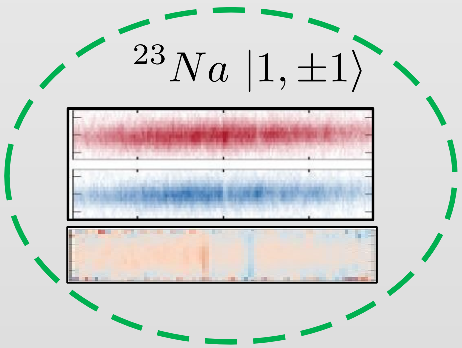

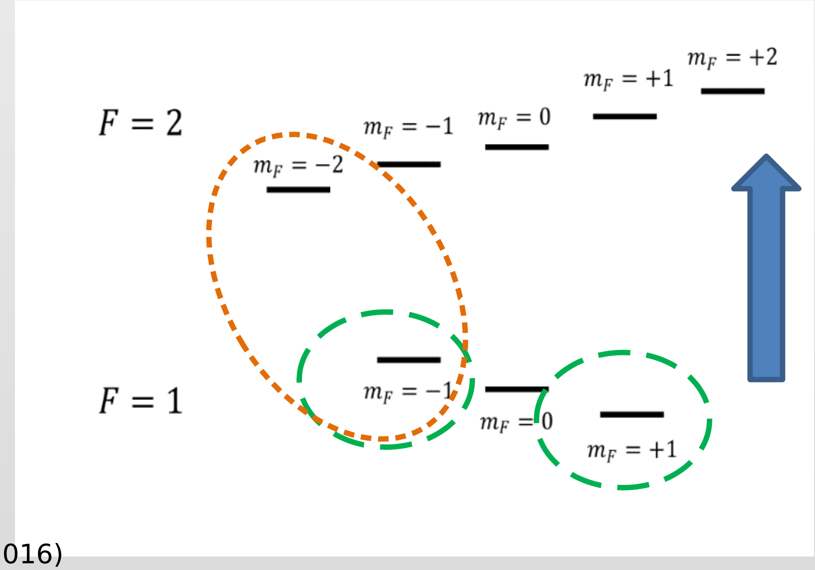

bias
B field

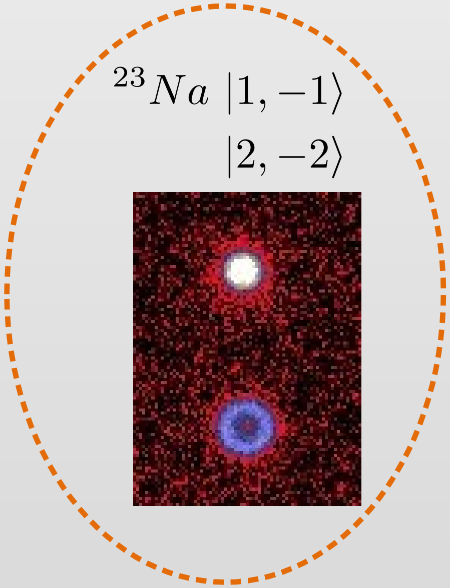

T. Bienaimé et al., PRA 94, 063652 (2016)
E. Fava et al,. PRL 120, 170401 (2018)
A. Farolfi et al., PRL 125, 030401 (2020)
A. Farolfi et al., PRA 104, 023326 (2021)
A. Farolfi et al., Nat. Phys. 17 1359 (2021)
R. Cominotti et al., PRL 128, 210401 (2022)

R. Cominotti et al., arXiv:2209.13235, PRX in press
A. Zenesini et al., arxiv:2305.05225

Mapping the mixture state on the Bloch sphere

$$i\hbar\partial_t\psi_1 = \left\{ -\frac{\hbar^2}{2m}\partial_x^2 + V + g_{11}|\psi_1|^2 + g_{12}|\psi_2|^2 \right\}\psi_1 - \frac{\hbar\Omega}{2}\psi_2$$

$$i\hbar\partial_t\psi_2 = \left\{ -\frac{\hbar^2}{2m}\partial_x^2 + V - \delta(t) + g_{22}|\psi_2|^2 + g_{12}|\psi_1|^2 \right\}\psi_2 - \frac{\hbar\Omega}{2}\psi_1$$

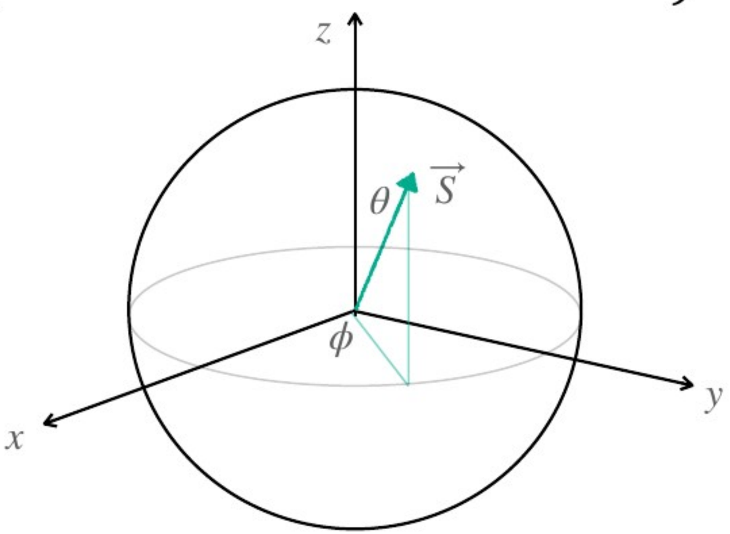

δ is the detuning of the coherent coupling

Ω is the strength of the coupling

ϕ is the relative phase

$Z = \dfrac{n_1 - n_2}{n_1 + n_2} = \cos\theta$ is the magnetization

$$\Delta = \frac{g_{11} - g_{22}}{2} < 0$$

$$\kappa = \frac{g_{11} + g_{22}}{2} - g_{12} < 0$$

$$\begin{aligned}\vec{S} &= \left(Re(\psi_1^*\psi_2), Im(\psi_1^*\psi_2), n_1 - n_2 \right) \\ &= n\left(\sin\theta\cos\phi, \sin\theta\sin\phi, \cos\theta \right)\end{aligned}$$

Spin dynamics on the Bloch sphere

$$i\hbar\partial_t\psi_1 = \left\{ -\frac{\hbar^2}{2m}\partial_x^2 + V + g_{11}|\psi_1|^2 + g_{12}|\psi_2|^2 \right\}\psi_1 - \frac{\hbar\Omega}{2}\psi_2$$

$$i\hbar\partial_t\psi_2 = \left\{ -\frac{\hbar^2}{2m}\partial_x^2 + V - \delta(t) + g_{22}|\psi_2|^2 + g_{12}|\psi_1|^2 \right\}\psi_2 - \frac{\hbar\Omega}{2}\psi_1$$

- External field contains a term that depends on the spin state (due to non-linearity)

$$\vec{H} = \Omega\hat{x} + \left[\delta_{eff} + \kappa n Z\right]\hat{z} \qquad \delta_{eff} = \delta + \Delta n$$

$$\mathscr{H} = -\vec{H}(\vec{S})\cdot\vec{S}$$

- Dynamics is precession about the vector $\vec{H}$, but different behaviour depending on the parameters

$$\partial_t\vec{S} = \vec{H}(\vec{S})\times\vec{S}$$

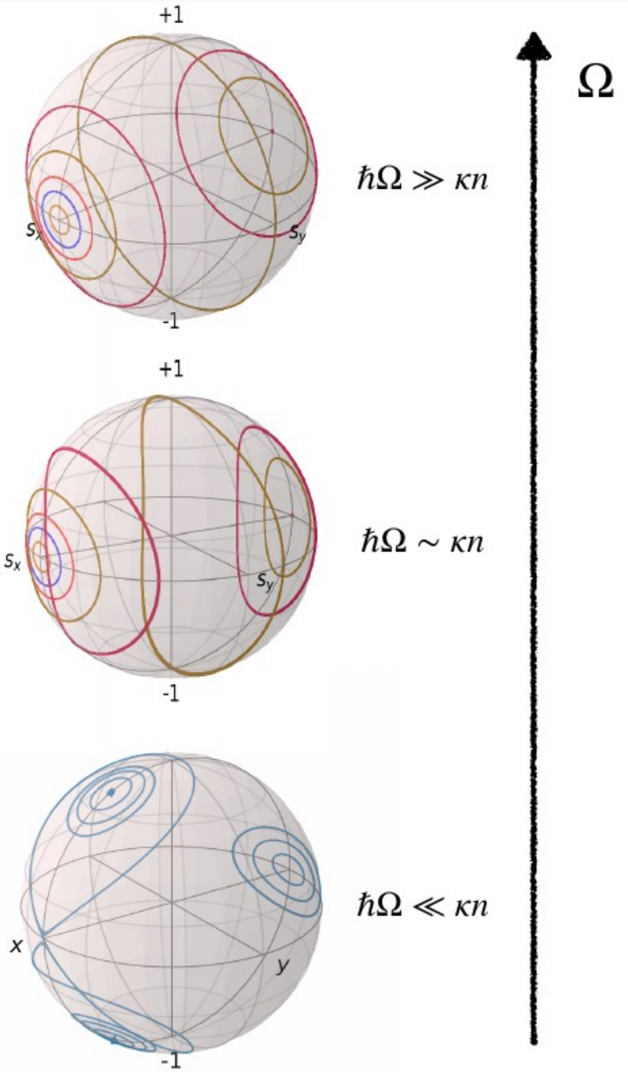

Physical Quantity	Magnetic System	Atomic System
Anisotropic Interactions	αn	κn
Axial field	B_3	$\delta_{\rm eff} = \delta_B + n\Delta$
Transverse field	B_1	$\Omega_{\rm R}$
Spin States	$\vert\uparrow\rangle$ $\vert\downarrow\rangle$	$\vert 2,-2\rangle$ $\vert 1,-1\rangle$
Magnetization Relative Magnetization	$\mathbf{S}(\vert\mathbf{S}\vert = n)$ $Z = S_3/n$	

Mapping between magnetic and atomic system.

equation of state para-ferro superfluid

$$E(Z,\phi) \propto -B_3 Z - \frac{|\alpha| n}{2} Z^2 - B_1 \sqrt{1-Z^2}\cos\phi$$

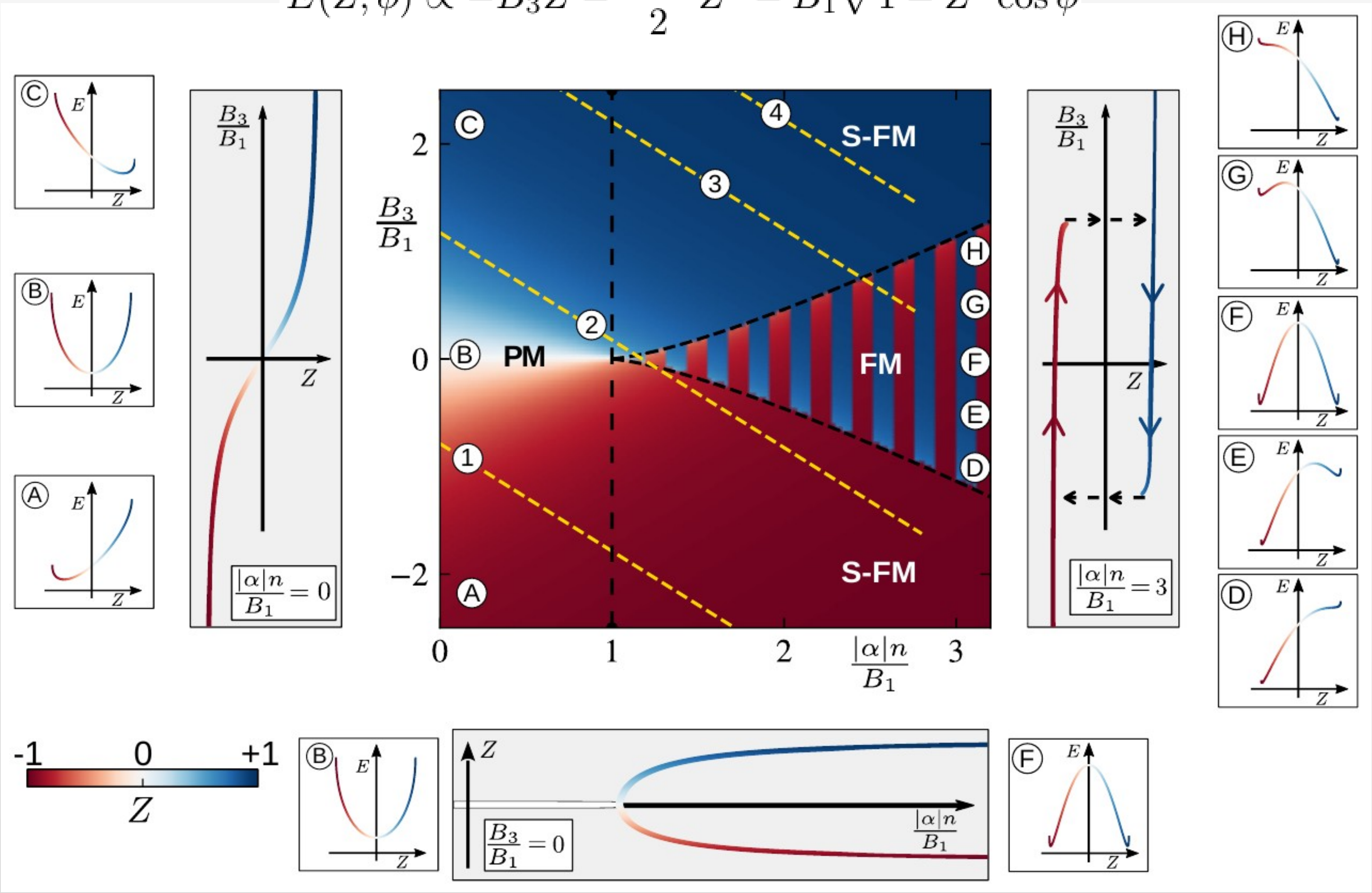

The experiment

- The gas is harmonically-trapped in an elongated potential: - not homogeneous density
  - the magnetic description is effectively 1D

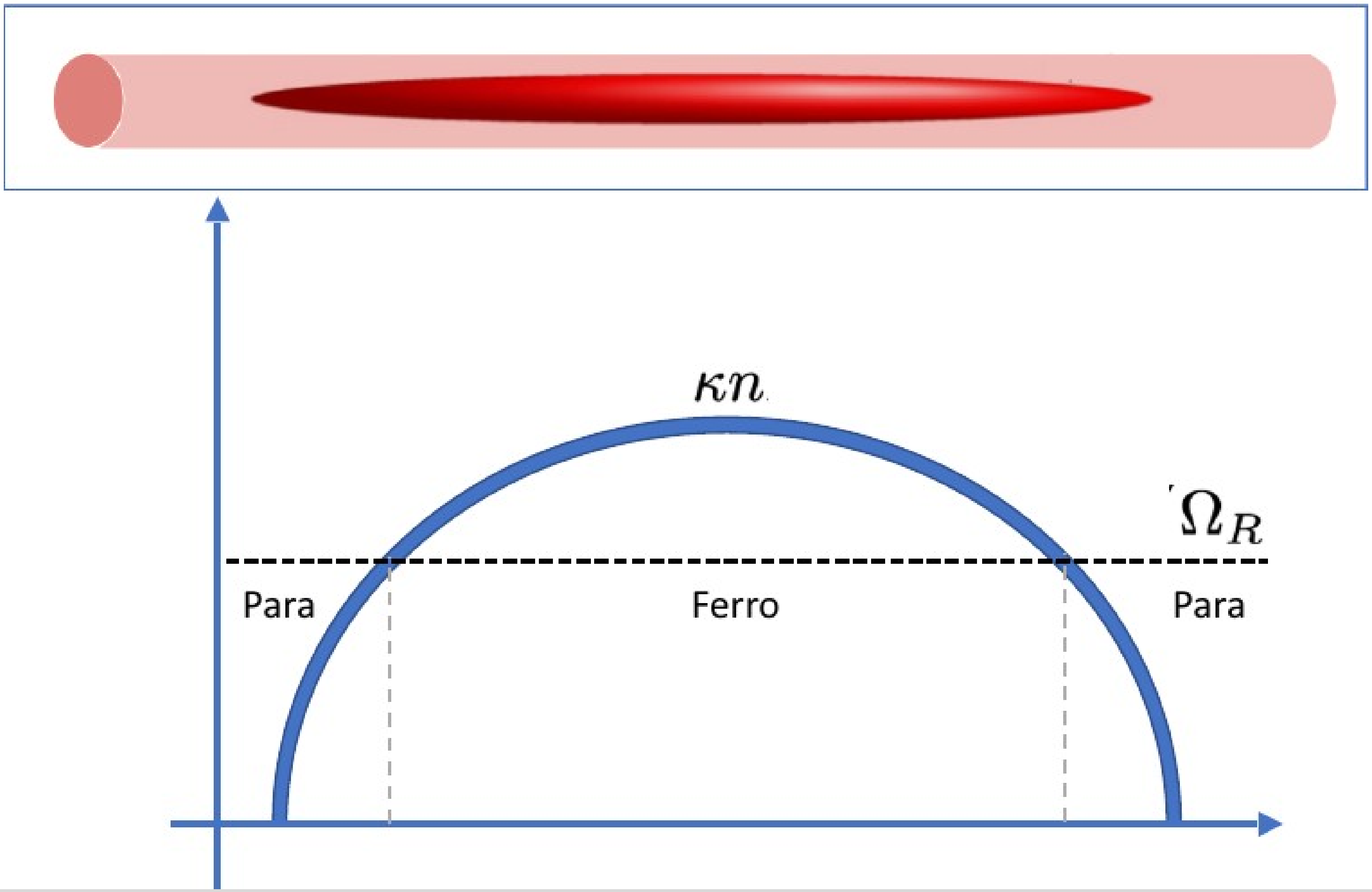

Magnetic field stability

Strict requirements on the stability of the magnetic bias field

to keep spin coherence

to probe spin manybody physics

$$\mu_B \, \delta B \ll \hbar\Omega < n|g_{12} - g| \ll ng$$

		60 nK	850 nK
10 - 50 Hz	200 Hz 1 kHz	1.2 kHz	17 kHz
5 - 25 μG			

Magnetic field stability

Characterization via atomic spectroscopy on a cold Sodium gas

Ramsey Spectroscopy

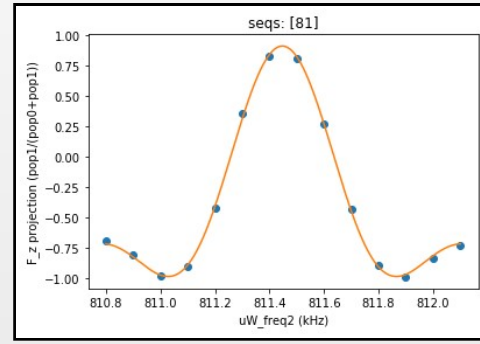

4-layer of mu-metal

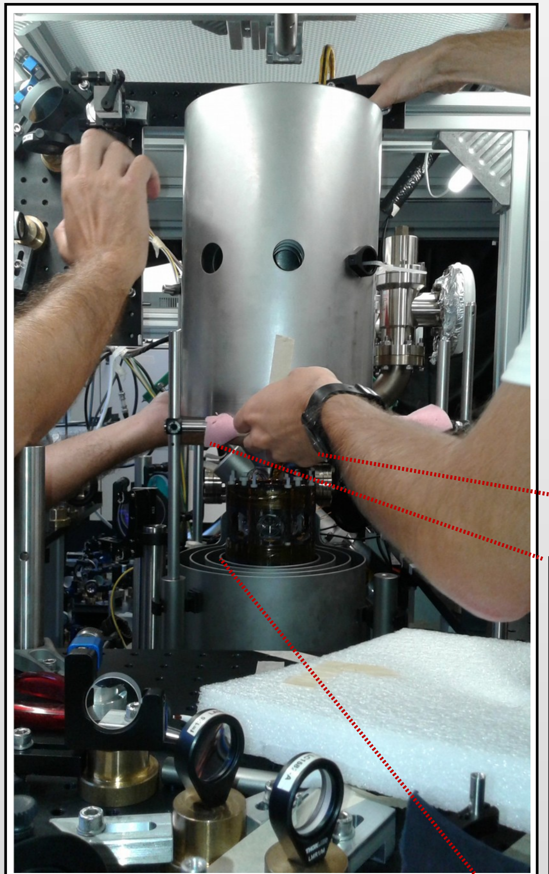

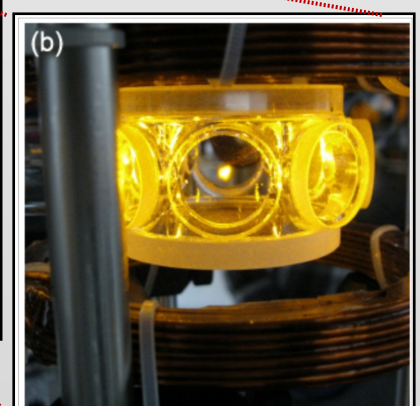

fluctuations attenuation: 10^5

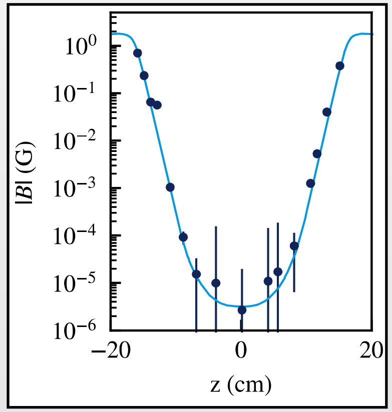

B Field stability:
a few μG over an hour

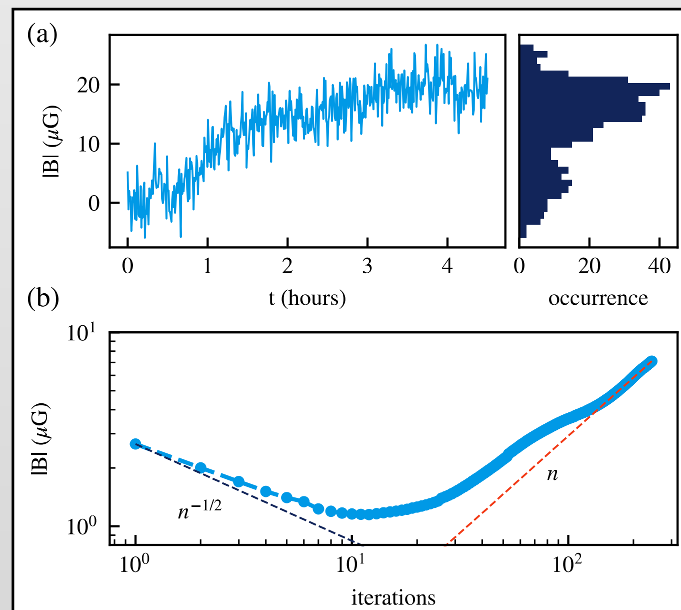

Farolfi *et al.*, RSI **90**, 115114 (2019)

Experimental protocol: spin rotation

Slow rotation of the spin by slowly changing the detuning and keeping the system close to one of its stationary states (either the ground state or the relative minimum)

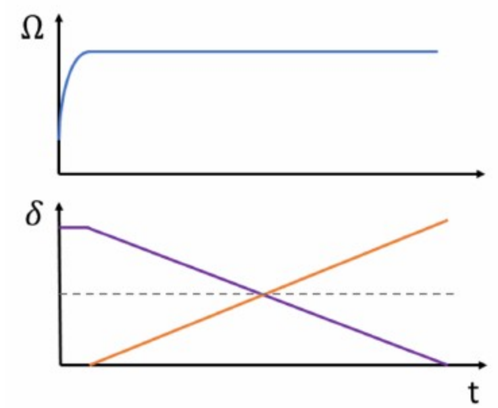

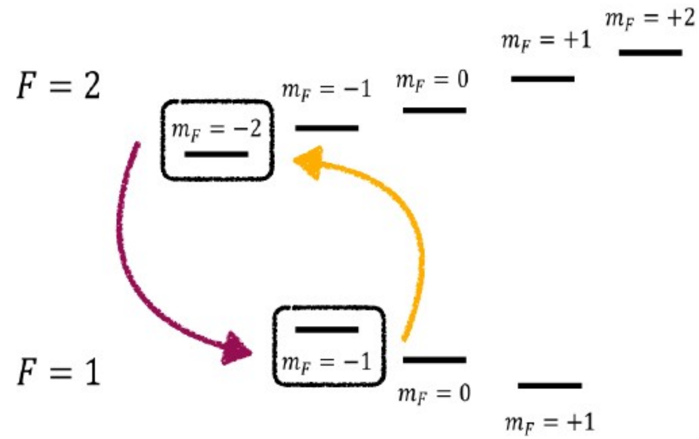

F=2

F=1

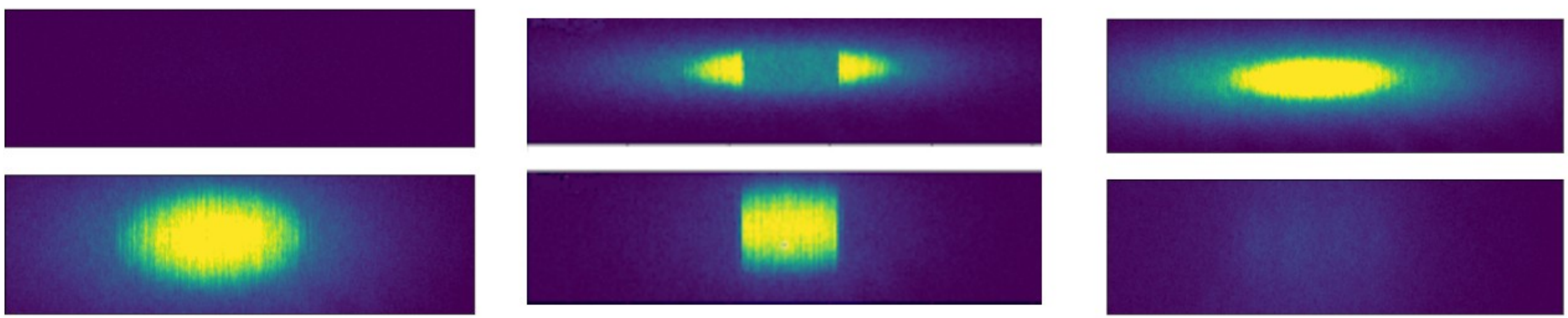

$\delta_{eff} \ll 0$ $\delta_{eff} \simeq 0$ $\delta_{eff} \gg 0$

spin rotation: measurements

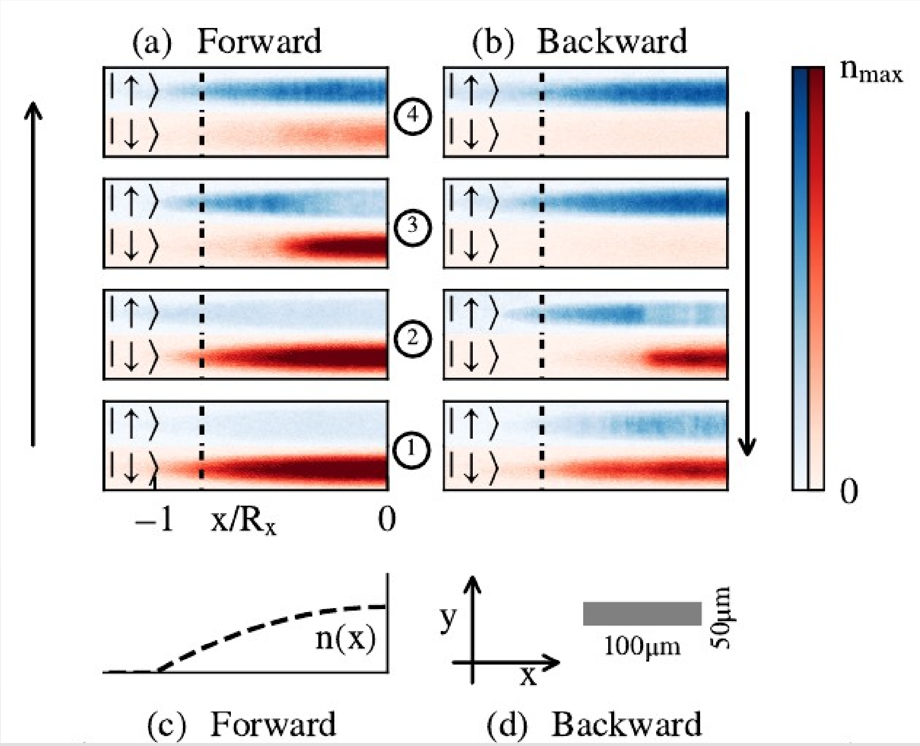

different state for same arrival point but different history

HYSTERESIS

measurement of the phase diagram

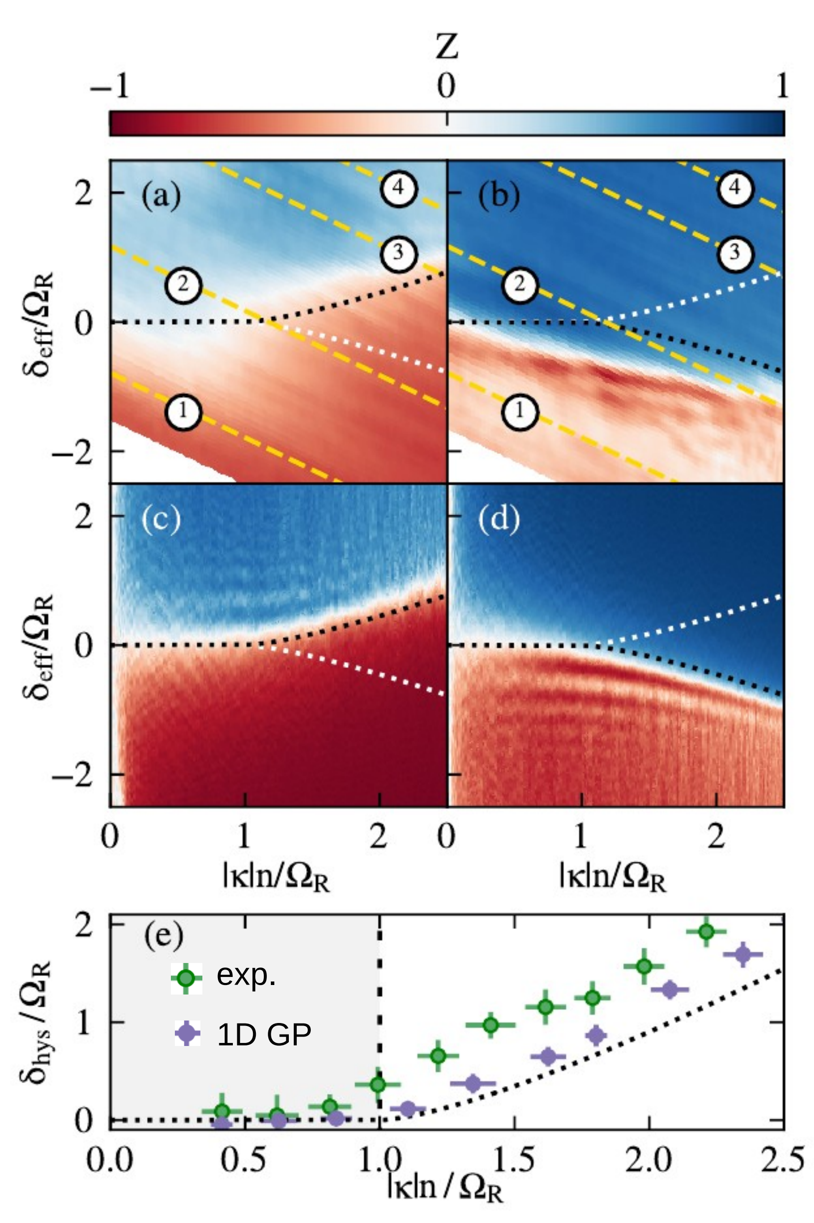

different state for same arrival point but different history

HYSTERESIS

- 1D GP simulations are qualitative agreement with the experiment.
- Better quantitative agreement between measurements and simulation extending to 2D.

R. Cominotti et al., arXiv:2209.13235, PRX in press

Characterization of the phase transition

Susceptibility

$$\chi = \frac{\partial Z}{\partial \delta_{\mathrm{eff}}}\bigg|_{\delta_{\mathrm{eff}}=0}$$

Fluctuations

$$\sigma^2$$

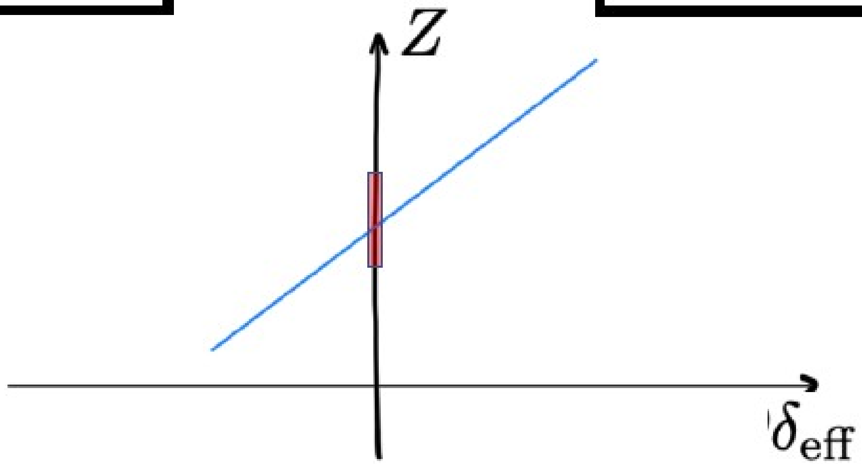

Both supposed to diverge at resonance
Different for quantum and thermal regime

Susceptibility and Fluctuations

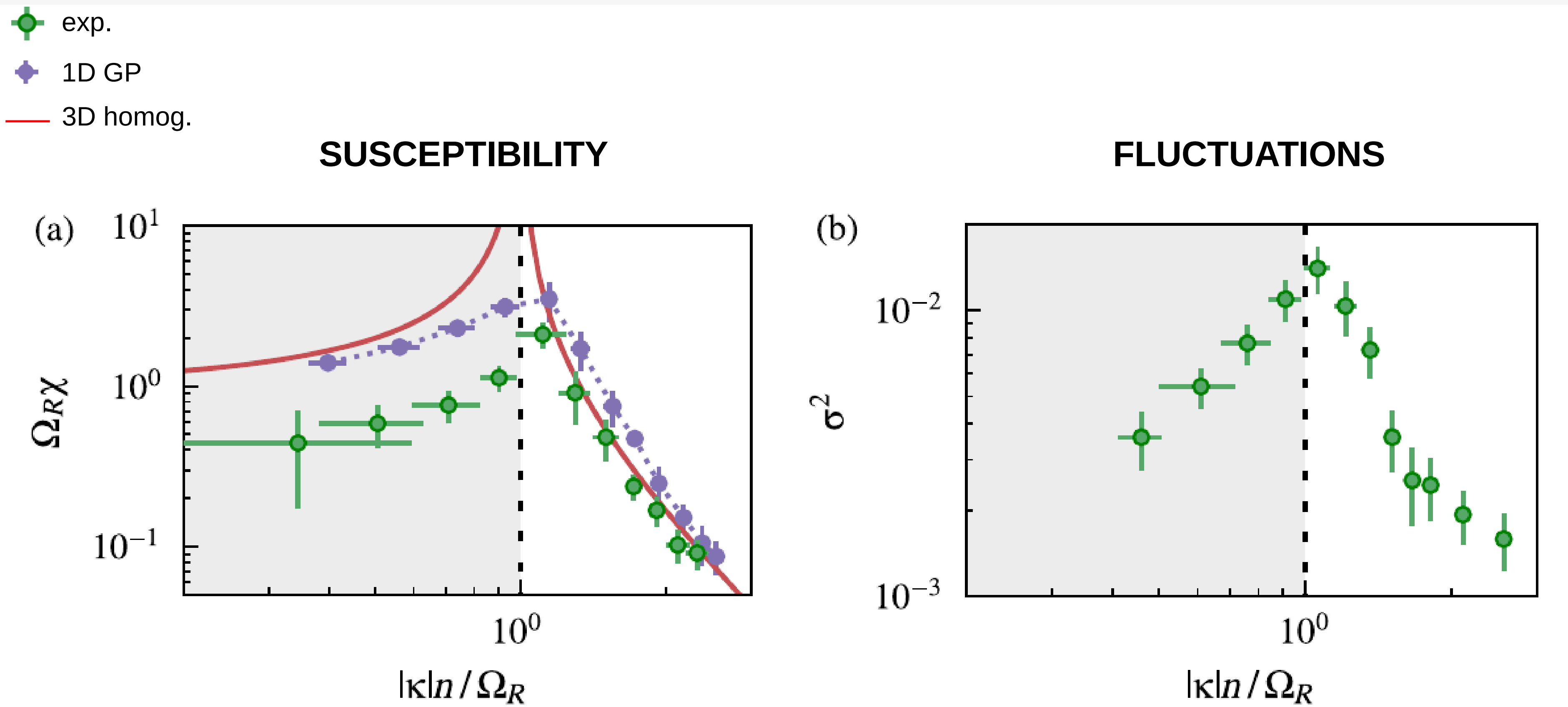

NOTE: accurate measurements of the susceptibility and of the fluctuations would open to tests of the fluctuation-dissipation theorem in the quantum regime.

Quantum simulation of Quantum Field Theories:

observation of False Vacuum Decay

Fate of a metastable ferromagnet

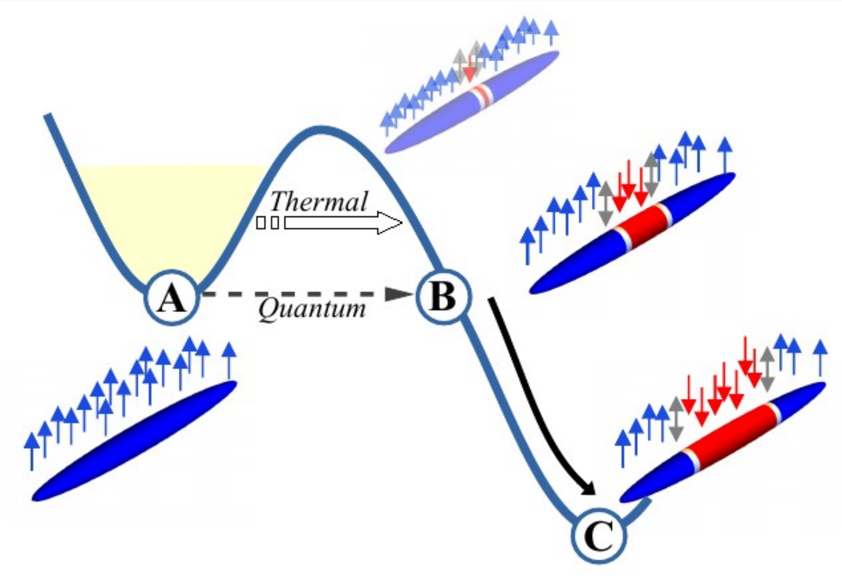

- The ferromagnetic magnetic superfluid is a field and may be prepared in a metastable state.

Key ingredients to observe **False Vacuum Decay**

- energy barrier originated by a nonlinear mean-field term
- exponential decay through nucleation of bubbles on an effective relativistic field,
- nucleation via quantum (or thermal quantum, many-body) tunneling through a potential barrier.

Bubble formation:
rate of bubble nucleation

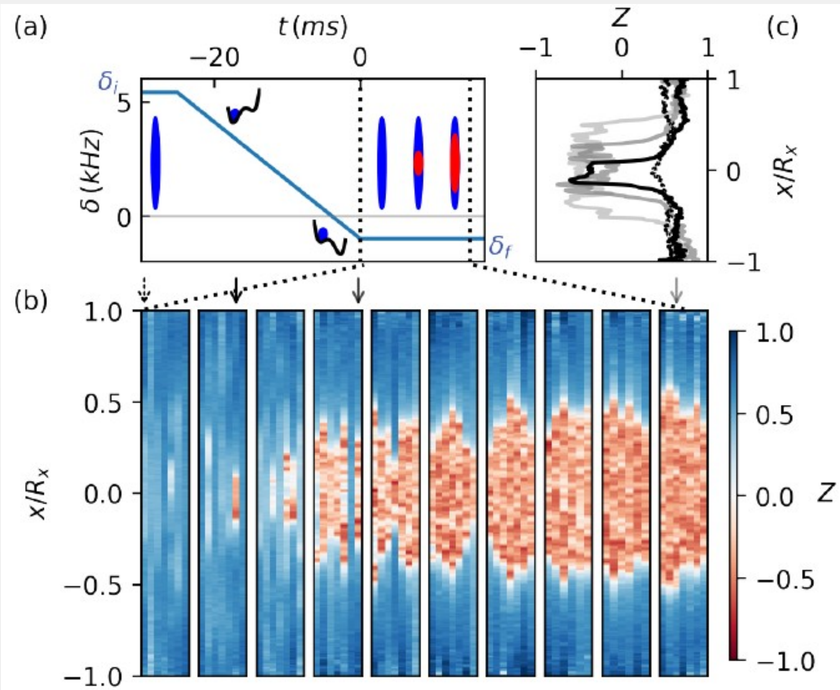

Probability of bubble nucleation

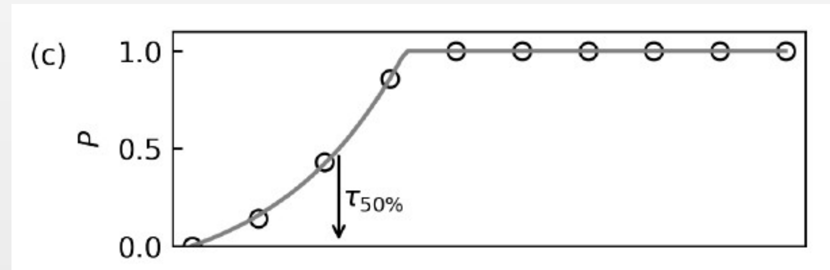

Average size of the bubble when present

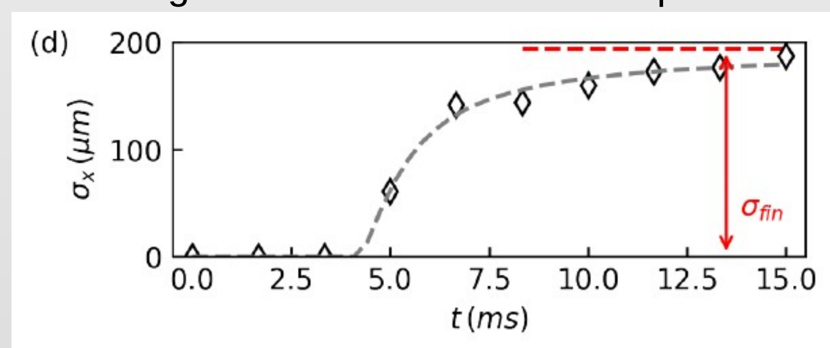

Experimental criterion for the identification bubble nucleation:

presence of a negative magnetization in the center of the sample.

The asymptotic size of the bubble is consistent with the absolute ground state of system.

A. Zenesini et al., arxiv:2305.05225

Decay of the averaged magnetization

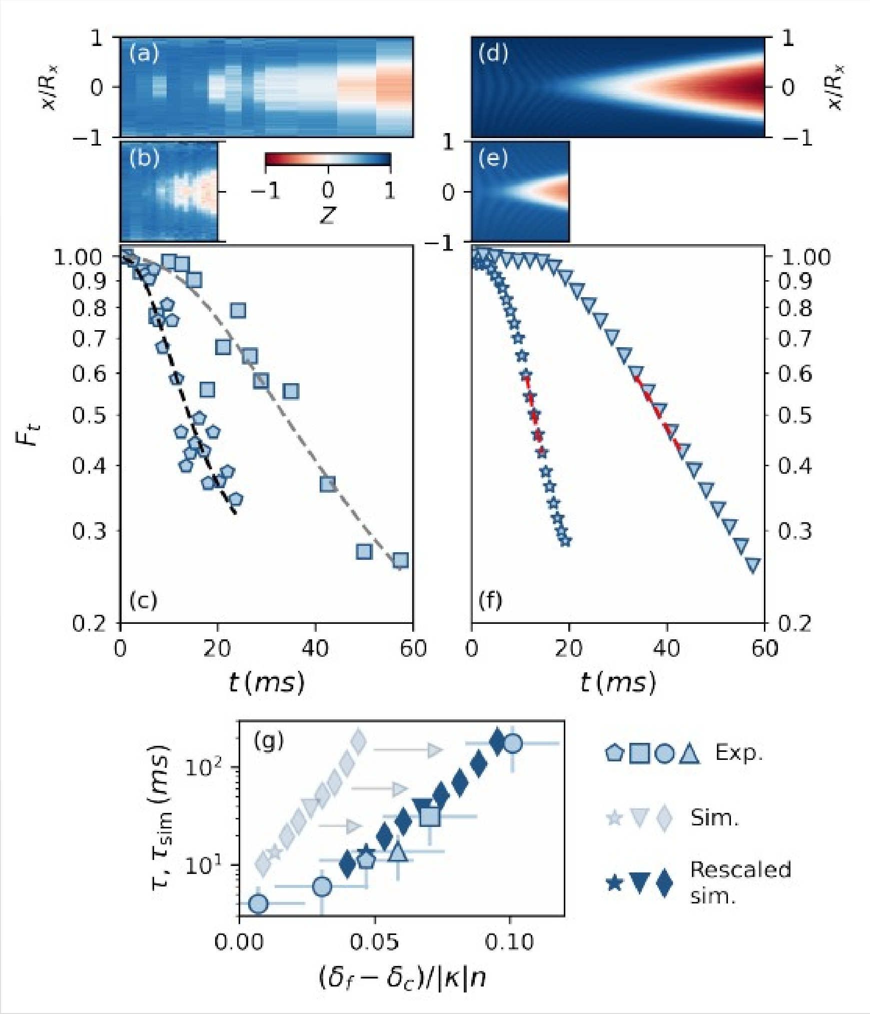

A. Zenesini et al., arxiv:2305.05225

False vacuum decay in quantum spin chains

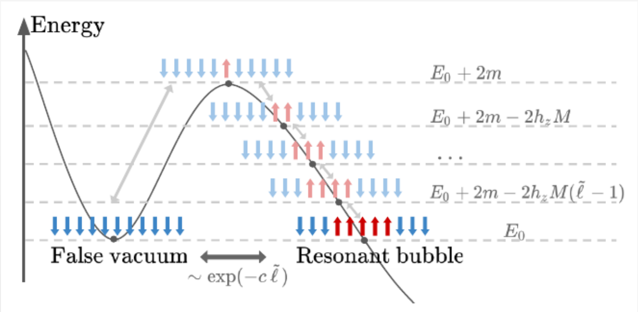

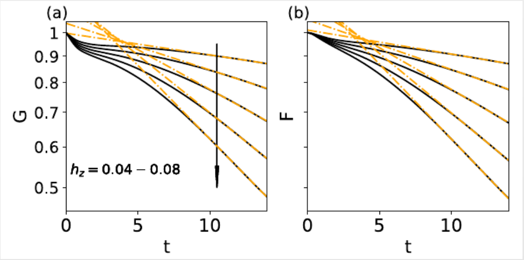

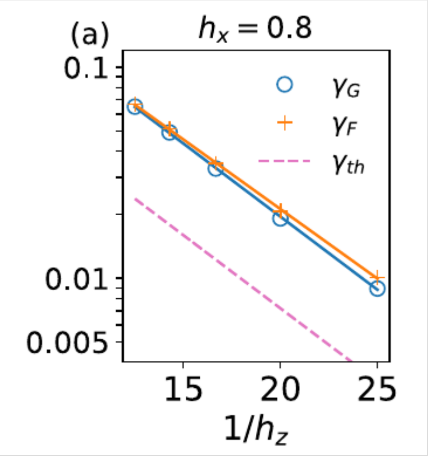

G. Lagnese et al., PRB B 104, L201106 (2021)

Bubble formation:
rate of bubble nucleation

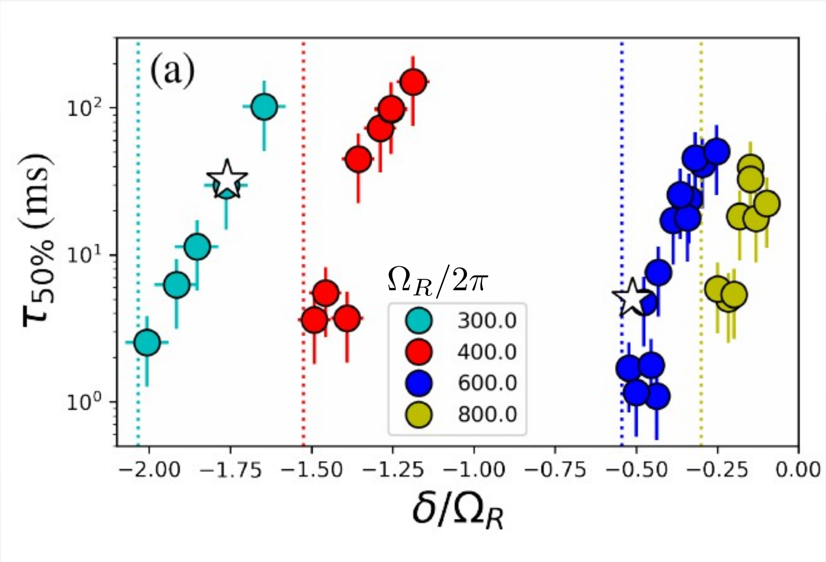

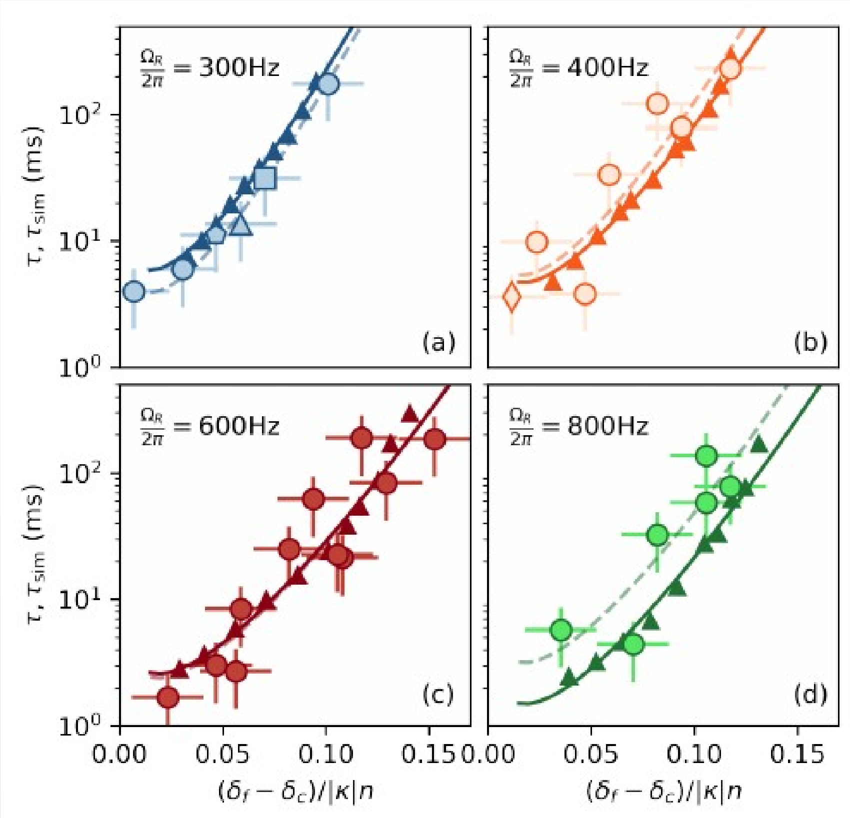

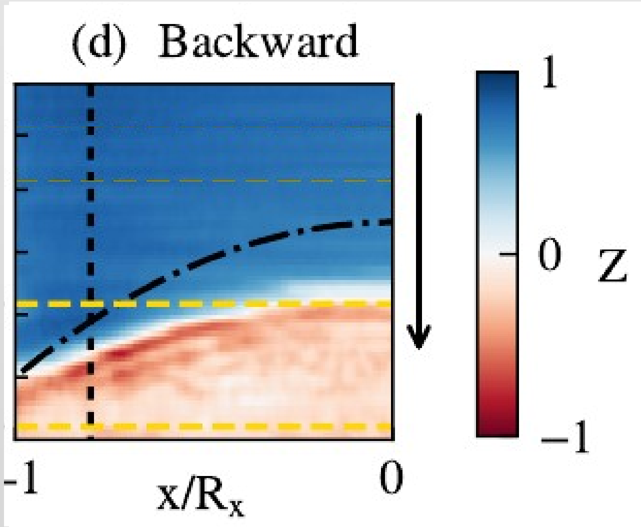

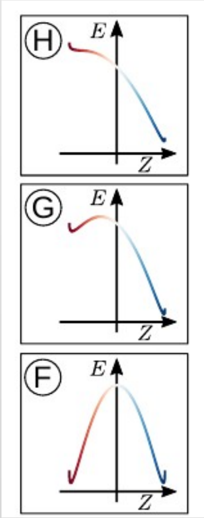

- $\delta_{\rm crit}$ is the detuning for the onset of the spin-jump in the hysteresis cycle.
- The fits of the 1D instanton provide correct order of magnitude of atom number and temperature.

A. Zenesini et al., arxiv:2305.05225

Conclusions and outlook

- Observation of the para- to ferro-magnetic phase transition in a superfluid.
- Deterministic production and control of domain walls in the superfluid ferromagnet.
- Generation of bubbles via macroscopic tunneling in the metastable ferromagnetic superfluid: preliminary indications of vacuum decay at finite temperature.finite temperature, etc.).

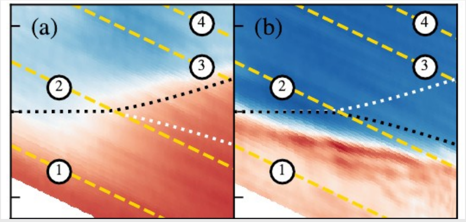

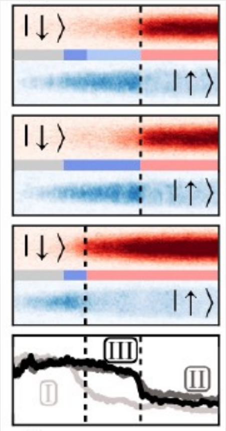

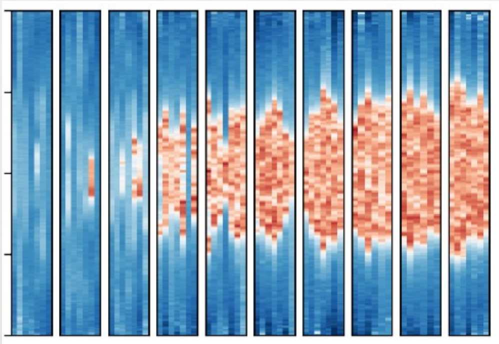

Open problems:

- Role of temperature on the phase transition, thermalization dynamics (T_{in}=0).
- Relaxation dynamics of the magnetic domain wall in the superfluid.
- Bubble nucleation rate: role of dimensionality, temperature, etc…
- Entanglement of a large number of atoms via bubble generation in zero dimension.

.

Fundamental excitations in a ferromagnet

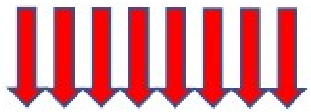

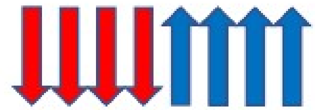

Creation
by passing through a phase transition (KZ) or
deterministically

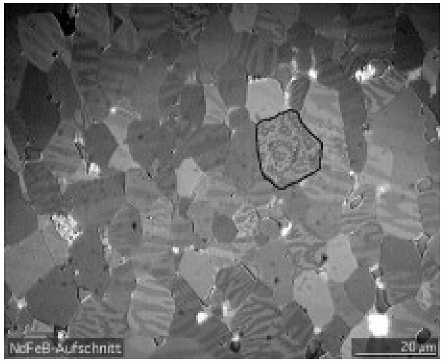

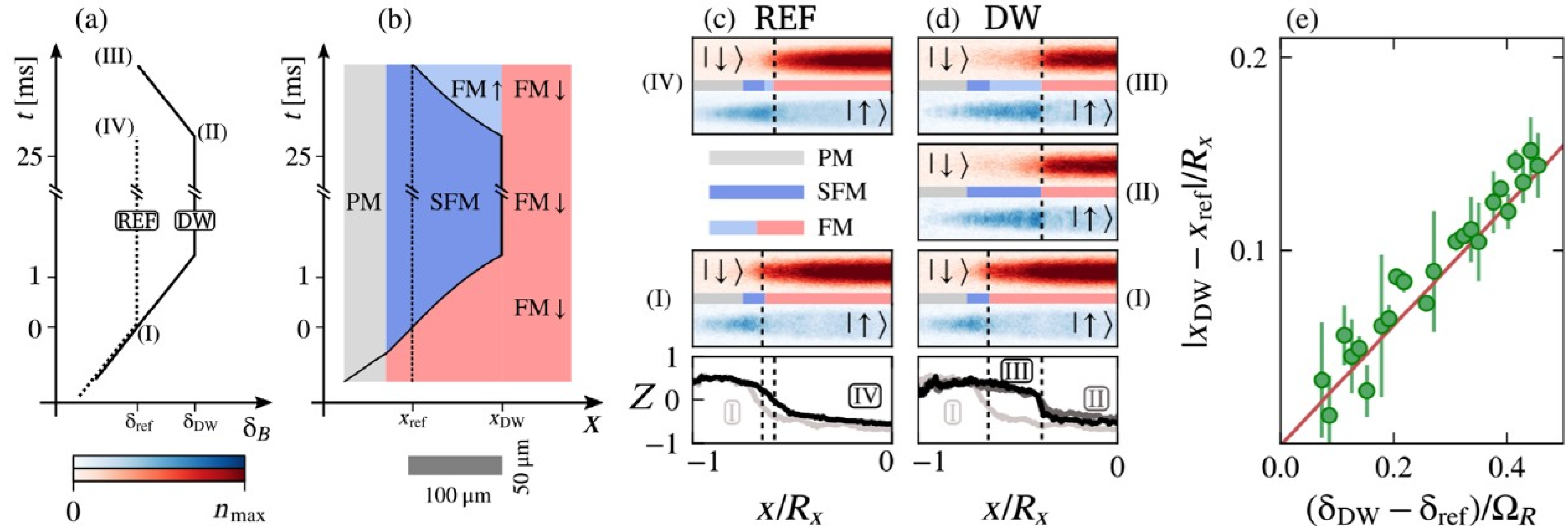

R. Cominotti et al., arXiv:2209.13235, PRX in press

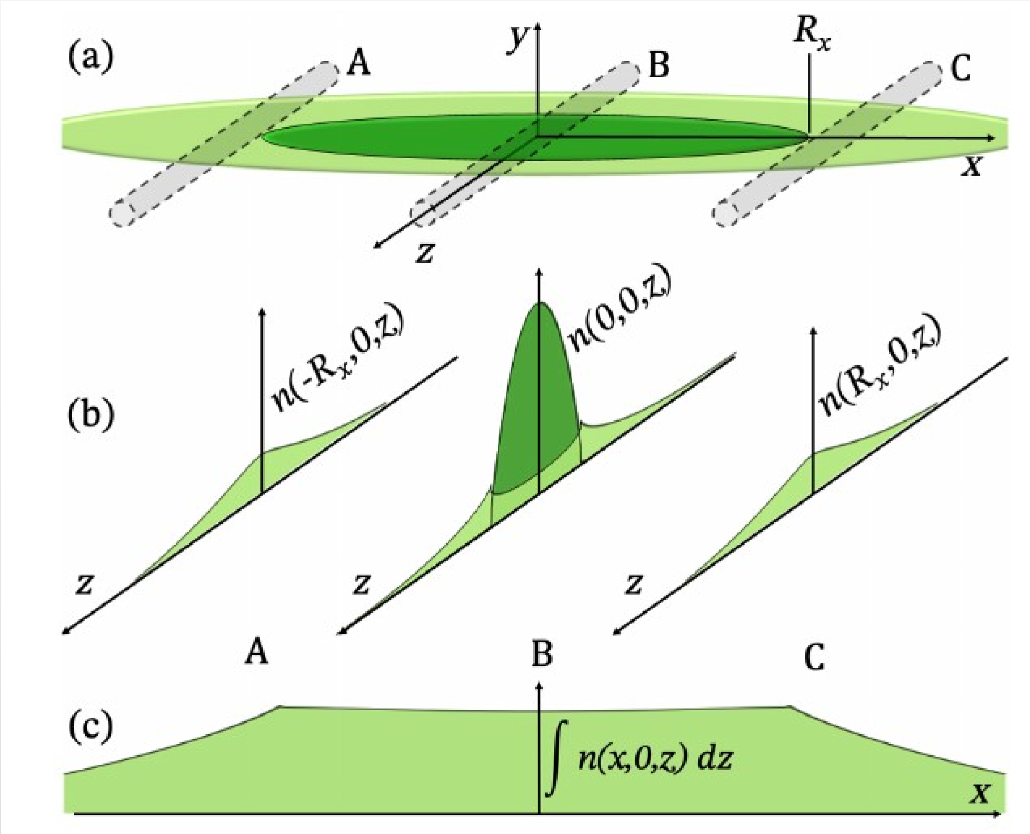
(a)
A
B
C
y
R_x
x
z
(b)
$n(-R_x,0,z)$
$n(0,0,z)$
$n(R_x,0,z)$
z
z
z
A
B
C
(c)
$\int n(x,0,z)\,dz$
x

spin rotation: measurements

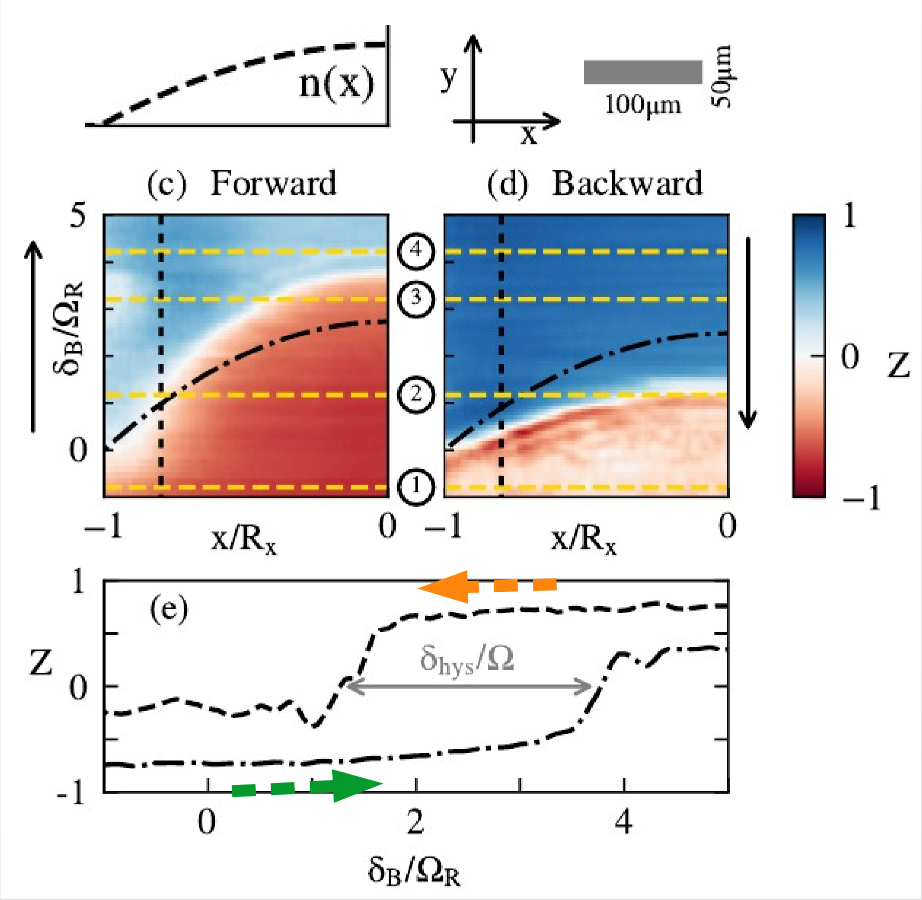

different state for same arrival point but different history

HYSTERESIS

R. Cominotti et al., arXiv:2209.13235, PRX in press

Spin temperature estimation

- Estimate a range for an effective 1D temperature of the mixture by comparing the results of numerical TW simulations with experimental data:
  - if T is too small, contrast is too good
  - if T is too large, spin modes are excited even before crossing the critical point.

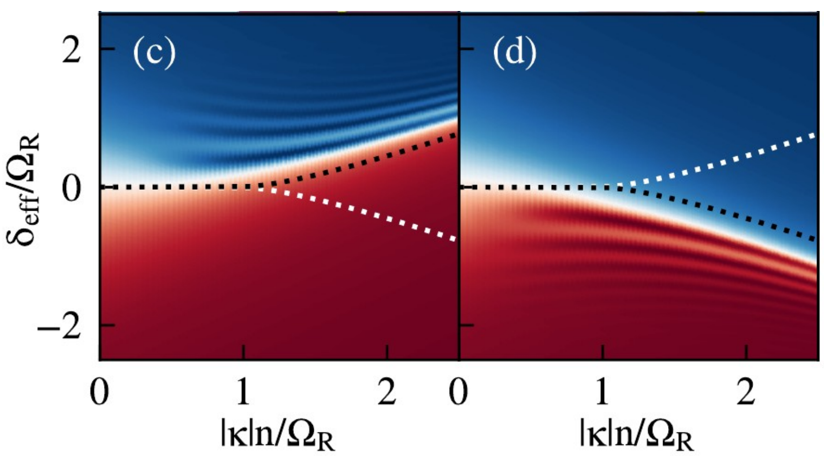

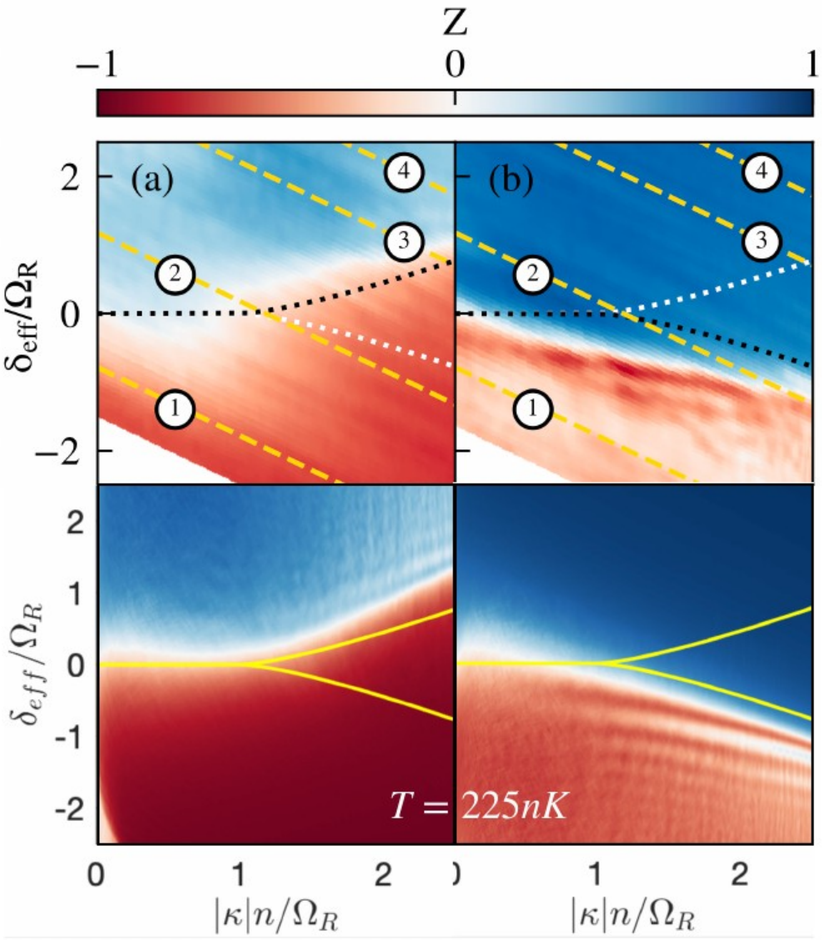

R. Cominotti et al., arXiv:2209.13235, PRX in press

Bubble formation: experimental protocol

- In the spin-polarized sample the metastable state is prepared via detuning ramps of the Rabi-coupled BEC.
- Metastability is reached in the central part of the cloud only due to the density dependent frequency offset.